Physical Processing – Part B
Separation

Course notes TU Delft, TA3390 part B

Revised and extended November 2011

Lectured by Dr. ir. R. Chaigneau

Cross belt magnetic separator.

Table of contents

CHAPTER 1. The flow of objects through fluids.

1.1 Introduction

Many processes for the separation of particles depend on the variation in the behaviour of the particles, when they are subjected to the action of the moving liquid.
In 1851, Stokes [1.1] calculated from purely theoretical considerations, the drag force exerted on a sphere moving at low velocity (laminar flow) in an infinite extent of continuous fluid:

$$F_d = 3\pi\mu d\nu \tag{1.1}$$

where F_d = the drag force (N)
μ = viscosity of the fluid (Ns/m^2)
d = diameter of the sphere (m)
ν = velocity of the fluid relative to the particle (m/s)

In describing physical transport phenomena, it is common to introduce a dimensionless friction factor f, or drag coefficient, which is defined as:

$$f = \frac{F_d}{EA} \tag{1.2}$$

where E is the characteristic energy per unit volume of fluid and A the characteristic area on which the force is considered to act.
The characteristic energy can be taken as:

$$E = \frac{1}{2}\rho_f \nu^2 \tag{1.3}$$

where ρ_f is the fluid density.
The area of a sphere is:

$$A = \frac{1}{4}\pi d^2 \tag{1.4}$$

hence equation (1.2) becomes for laminar flow (Re<2):

$$f = \frac{24}{\mathrm{Re}} \tag{1.5}$$

where

$$\mathrm{Re} = \frac{\rho_f \nu d}{\mu} \tag{1.6}$$

is the particle Reynolds number.

At high Reynolds numbers (Re>500, turbulent flow), the flow around the particle shows a constant drag coefficient:

$$f \approx 0.44 \tag{1.7}$$

Between the laminar and turbulent regions is a transition zone, where the drag coefficient can be approximated by:

$$f \approx \frac{18.5}{\mathrm{Re}^{0.6}} \tag{1.8}$$

When it is assumed that the settling of a particle is not hindered by the presence of other particles, then expressions can be derived for the terminal falling velocity v_0 of the particle.
When the terminal falling velocity of the particle is reached, drag force, gravity and buoyancy force are in equilibrium:

$$F_d = F_g + F_b \tag{1.9}$$

or

$$f \cdot \frac{1}{2}\rho v_0^2 \cdot \frac{1}{4}\pi d^2 = \frac{1}{6}\pi d^3(\rho_s - \rho_f)g \tag{1.10}$$

from which

$$v_0^2 = \frac{4d(\rho_s - \rho_f)g}{3f\rho_f} \tag{1.11}$$

where ρ_s = particle density
g = gravity acceleration

In the laminar region, f = 24/Re. Substitution in equation (1.11) yields:

$$v_0 = \frac{1}{18}\frac{d^2(\rho_s - \rho_f)g}{\mu} \tag{1.12}$$

Equations for the other flow regions can easily be obtained by substitution of the appropriate equation for f in equation (1.11).
In systems where centrifugal acceleration is present rather than gravitational acceleration, the equations can be rewritten by replacing the gravitational acceleration g by the centrifugal acceleration $\omega^2 r$, where r is the radius of rotation and ω the angular velocity.

Example 1.1

What will be the setting velocity of a 0.4 mm spherical steel particle with density 7870 kg/m^3? The oil density is 820 kg/m^3 and the viscosity 0.01 Ns/m^2.

Solution:

$$v_0 = \frac{1}{18}\frac{(0.4*10^{-3})^2(7870-820)9.81}{0.01} = 0.061\, m/s$$

Check:

$$\mathrm{Re} = \frac{\rho v_0 d}{\mu} = \frac{820*0.061*0.4*10^{-3}}{0.01} = 2.0$$

hence the flow conditions are laminar.

Example 1.2

A spherical sand particle with density 2750 kg/m^3 settles freely in water. If the particle Reynolds number is 0.1, calculate the particle diameter. The viscosity of water is 0.001 Ns/m^2, the density 1000 kg/m^3.

Solution:
Using equation (1.12) gives:

$$v_0 = \frac{1}{18}\frac{d^2(2750-1000)9.81}{0.01} = 9.5410^5 d^2\, m/s$$

The Reynolds number then becomes:

$$\mathrm{Re} = \frac{1000*9.5410^5*d^2*d}{0.001} = 0.1$$

from which d = 4.76 10^{-5} m.

In many cases, the flow regime of a freely settling particle is not known at the start of the calculation. If it is not known whether the flow is laminar, turbulent or in the transition zone, the terminal falling velocity can be found by computing first:

$$\mathrm{Re}^2 f(\mathrm{Re}) = \frac{2\rho_f d^2}{\mu^2 A}F_d = \frac{4d^3\rho_f(\rho_s-\rho_f)g}{3\mu^2} \quad \text{(for a sphere)} \qquad \textbf{(1.13)}$$

Then the Reynolds number can be read from a graph of $Re^2f(Re)$ against Re (Figure 1.1) and the terminal falling velocity is given by

$$v = \frac{\mu \mathrm{Re}}{\rho_f d} \tag{1.14}$$

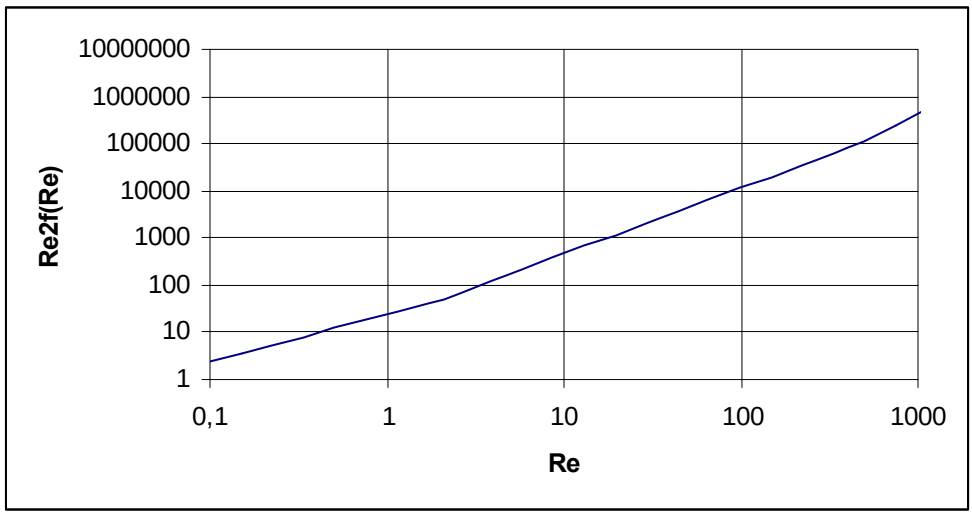

Figure 1.1 Graph of $Re^2f(Re)$ against Re for spherical particles.

1.2 *Effect of shape and orientation on drag*

A spherical particle is unique in that it presents the same surface to the oncoming fluid, whatever its orientation. For non-spherical particles, however, the orientation must be specified before the drag force can be calculated.
The experimental data for drag can be correlated in the same way as for the sphere by plotting the drag coefficient f against the Reynolds number.
The diameter of the particle is now defined as the diameter of the circle, having the same area as the projected area of the particle, and is therefore a function of the orientation, as well as the shape of the particle.
The curve for f against Reynolds can be divided again in a laminar region, turbulent region and transition region.
In the laminar region, the flow is entirely streamlined and practical data suggests a correlation of the form:

$$f = \frac{K}{\mathrm{Re}} \tag{1.15}$$

The constant K varies somewhat according to the shape and orientation of the particle, but always has a value of about 24.
In this region, a particle falling freely under the action of gravity will normally move with its longest surface parallel to the direction of motion. In the transition region, a freely falling particle will tend to change its orientation as the value of the Reynolds number changes and some instability may be apparent. In the turbulent region, the particle will tend to fall so that

it is presenting the maximum possible surface to the oncoming fluid. Typical values of f in this region are shown in Table 1.1.

Thin rectangular plates, planes perpendicular to direction of motion		
length/width = 1-5	f =	1.2
20		1.5
infinity		1.9
Cylinders with axes parallel to the direction of motion		
length/diameter = 1	f =	0.9
Cylinders with axes perpendicular to the direction of motion		
length/diameter = 1	f =	0.6
5		0.7
20		0.9
infinity		1.2

Table 1.1 Friction coefficient for non-spherical particles.

It should be noted that the friction coefficients for non-spherical particles are higher than the value 0.44 for a spherical particle.
Gas bubbles in a liquid can be considered spherical if they are very small (for water: smaller than 2 mm in diameter). In principle, the formulas for solid particles do not apply to a bubble because the liquid does not have the same velocity as the bubble at the interface (the so-called stick condition does not hold). However, deviations from the solid particle formulas are only observed in very pure liquids. In practical cases, the formulas will apply, because contaminants in the liquid will collect at the gas-liquid interface and simulate a "hard" shell, as with a solid particle.

1.3 *Other correction factors*

A number of other factors may have to be considered when treating the flow of particles through a fluid. The most important one is hindered settling, which will be discussed in a later chapter.
Although generally not important in full size operations, a wall effect may be significant in laboratory testing. This problem arises because the moving particle pulls fluid along with it, and in the vicinity of the stationary wall, the fluid movement is slowed, resulting in an apparent increase in drag coefficient.
The drag forces computed with formula 1.2 relate to steady motion, i.e. the particles are assumed to have constant speed. If the particles are accelerated, the difference between the gravity and buoyant force on the one hand and the drag force on the other is used for the acceleration of the particle and part of the fluid around it:

$$F_g + F_b - F_d = m_p a + m_f a \qquad \textbf{(1.16)}$$

where m_p = mass of particle
m_f = mass of accelerated fluid (added mass)

For laminar flow and spherical particles the volume of the fluid that is accelerated with the particle amounts to half the volume of the particle.

1.4 Fluidization and sedimentation

Hydrodynamically there is little difference between fluidization and sedimentation, both can be considered as an expanded packed bed where the particles are free to move relative to one another. Fluidization and sedimentation are distinguished by whether the fluid or solid moves relative to the containing vessel.

If a fluid is passed through a bed of unrestrained particles, the pressure drop will increase until a point is reached where the pressure drop and weight just counteract the buoyancy forces. Provided the bed is free flowing, it will start to behave like a boiling liquid. Such a bed is said to be fluidized.

If the fluid velocity is increased further, the bed continues to expand and eventually, as the terminal velocity is approached, the particles are entrained in the fluid.

The minimum fluidization velocity is the velocity where the bed just starts to be fluidized. Above this minimum velocity, the pressure drop increase is negligible as the velocity increases.

With smooth particles, the point of minimum fluidization is not a sharp feature. Irregularly shaped particles may cause a peak on the Δp-v curve, due to particle interlocking (dashed portion in Figure 1.2).

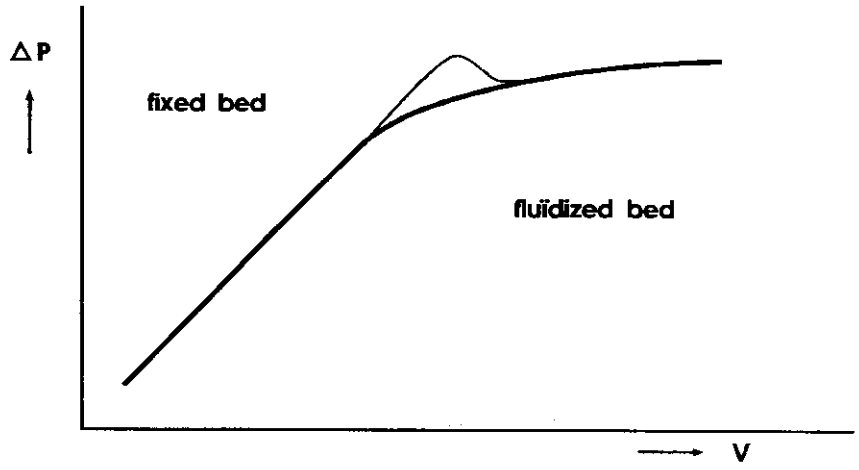

Figure 1.2 Pressure drop vs superficial velocity in a fluidized bed.

Sedimentation or hindered settling represents the opposite of fluidization. Generally the particles accelerate rapidly and settle at their terminal velocity, producing an interface between the clear liquid and the slurry. As the particles settle, an interface between settled and settling particles rises from the bottom. Eventually the two interfaces meet, after which the settled particles go through a process of compression, which involves very slow settling.

The pressure drop for flow through a fixed bed has been determined empirically. It can be described by the Ergun equation:

$$\frac{\Delta P}{H} = \frac{1-\varepsilon}{\varepsilon^3 d_{vs}}\left(\frac{150(1-\varepsilon)\mu v_s}{d_{vs}} + 1.75\rho v_s^2\right) \quad \textbf{(1.17)}$$

where ΔP = pressure drop
H = height of the bed
ε = volume of voids/volume of the bed
v_s = superficial velocity, the average linear velocity of the fluid if no particles were present
d_{vs} = the volume surface diameter of the particle = $6V_p/S_p$
V_p = volume of the irregular particle
S_p = surface area of the irregular particle

For the gas flow through a fluidized bed, an equation similar to the Ergun equation has been found:

$$\frac{\Delta P}{H} = \frac{1-\varepsilon}{\varepsilon^3 d_{vs}}\left(\frac{200(1-\varepsilon)\mu v_s}{d_{vs}} + 3.0\rho v_s^2\right) \quad \textbf{(1.18)}$$

An alternative and better approach to fluidization and sedimentation of uniform spherical particles is to use empirical relationships. One of the most widely known is the one by Richardson and Zaki [1.2,1.3]:

$$\frac{v_f}{v_0} = \varepsilon^n \quad \textbf{(1.19)}$$

where v_f = falling velocity of suspension with respect to a fixed horizontal plane (sedimentation), or superficial velocity (fluidization)
v_0 = terminal velocity of a single particle at infinite solution

The exponent n can be approximated by:

$$n = \frac{4.8}{2+\beta} \quad \textbf{(1.20)}$$

where β is the slope of the relationship of friction factor f versus Re_p, where

$$\mathrm{Re}_p = \frac{d\rho_f v_0}{\mu} \quad \textbf{(1.21)}$$

i.e. the Reynolds number based on terminal velocity.

For laminar flow, β=-1, hence n=4.8, resulting in

$$\frac{v_f}{v_0} = \varepsilon^{4.8} \quad \textbf{(1.22)}$$

1.4.1 **Flux curves**

In some situations, instead of considering the settling rate ν, it is more useful to consider the flow rate of particles per unit area, the solids flux ψ, which is given by:

$$\psi = C\nu \tag{1.23}$$

where ψ = mass flux of particles
C = concentration, mass per unit volume

Since $1 - C/\rho_s = \varepsilon$ and ν can be represented by equation (1.19), the solids flux becomes:

$$\psi = \nu_0(1-\varepsilon)\rho_s \tag{1.24}$$

which results in the characteristic flux curve for sedimentation, shown in Figure 1.3.

It can be seen that a low solids flux occurs at low solids concentrations, when few particles are present, and at high concentrations, when settling becomes severely reduced by hindrance effects.

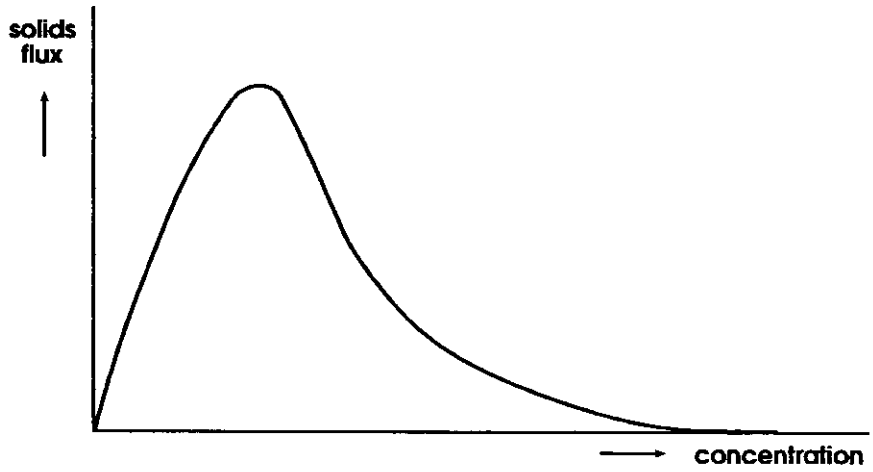

Figure 1.3 Sedimentation flux curve.

1.4.2 **Settling ponds**

Some mineral processing units behave like an ideal settling pond. Essentially this is a pond in which slurry is fed at the one side and the overflow at the other side of the pond contains a much lower solids content. This is illustrated in Figure 1.4.

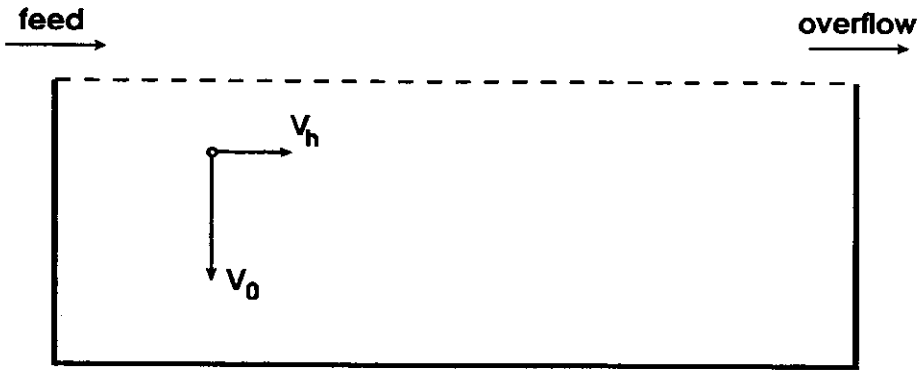

Figure 1.4 Velocity components of a particle in a settling pond.

The particles have a horizontal velocity component equal to the horizontal liquid velocity; they are also subjected to gravitational settling forces and thus have a vertical velocity component as well.
The limiting size of a particle is that which can just settle the depth of the pond during passage. The time t_0 to settle the depth H of the pond is:

$$t_0 = \frac{H}{v_0} \tag{1.25}$$

which is also equal to the residence time τ, the time to travel the length L of the pond:

$$\tau = \frac{L}{v_h} \tag{1.26}$$

However,

$$v_f = \frac{F_v}{WH} \tag{1.27}$$

where F_v = volumetric flow rate of the slurry
W = width of the pond
H = height of the pond

resulting in

$$v_0 = \frac{F_v}{WL} = \frac{Fv}{A_t} \tag{1.28}$$

where At = surface area of the pond.

This shows a significant feature of settling ponds; the ability to capture a particle is independent of the depth of the pond.
In practice, concentration gradients and non-ideal plug flow conditions will exist, resulting in a required area being greater than the conventional area. The areal efficiency η is defined as:

$$\eta = \frac{\text{theoretical surface area}}{\text{actual surface area}} * 100\% \qquad \textbf{(1.29)}$$

Values of η are usually in the order of 50-100%, at higher concentrations and flow rates, η may be significantly lower.

1.5 *Definition of velocities in particle/fluid systems*

In a vertical flow of particles, a number of velocities are commonly used, such as superficial velocity, interstitial fluid velocity, particle velocity, swarm velocity and slip velocity.
Three main types of vertical flow systems are being considered:

i) fluidization
ii) sedimentation
iii) combination of i) and ii)

In this section the particle and fluid velocities of each system will be defined.

1.5.1 **Liquid-solid fluidized systems**

Richardson and Zaki [1.2] gave the following definition of fluidization: "When a fluid is passed slowly through a bed of granular solids, the bed remains static. If the velocity is increased, a stage is reached when the particles reorientate themselves and present a greater cross-sectional area to the flow of fluid; this readjustment continues until the loosest stable arrangement is attained. With further increase, the particles are individually supported by the fluid, and the bed becomes fluidized. At velocities greater than the minimum required to produce fluidization, the bed continues to expand and the particles remain uniformly dispersed in the liquid."

In fluid/solid systems the following velocities can be distinguished:

v_d : Particle velocity with respect to the wall of the system.
u : Superficial fluid velocity with respect to the wall of the system.
i.e. the fluid velocity based upon the total cross section of the empty tube.
v_I : Interstitial fluid velocity with respect to the wall of the system.
i.e. the fluid velocity in the pores between the particles.
$u_v(\varepsilon)$: Velocity of a swarm of particles with porosity in absence of a superficial fluid velocity.
v_s : Slip velocity.
i.e. the relative velocity between particle and fluid.

In a fluidized bed the particle swarm is in equilibrium with the corresponding superficial fluid velocity, so the superficial fluid velocity u is equal to the value of the swarm velocity $u_v(\varepsilon)$ but in an opposite direction. The individual particle velocity $v_d = 0$. The interstitial fluid velocity v_i is equal to the superficial fluid velocity u divided by the open area between the particles, the porosity ε.

Velocities are vector quantities, so they have a length and a direction. The direction is given by a minus or plus sign, depending on the definition of the positive direction. It is possible that the scalar component of two velocities is equal but the orientation is different.

Now for a fluidized system the following equations can be defined:

$$v_d = 0 \qquad \textbf{(1.30)}$$

$$u \neq 0$$

$$v_i = \frac{u}{\varepsilon} \qquad \textbf{(1.31)}$$

$$v_s = v_d - v_i \qquad \textbf{(1.32)}$$

Combining equations (1.30) to (1.32) gives:

$$v_s = 0 - \frac{u}{\varepsilon} = -\frac{u}{\varepsilon} \qquad \textbf{(1.33)}$$

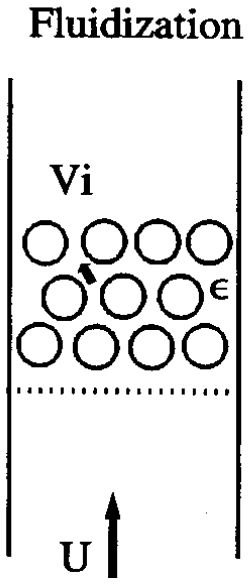

Figure 1.5 Velocities in a fluidized system

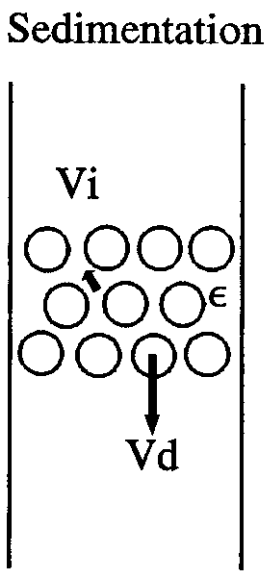

Figure 1.6 Velocities in a sedimentation system

1.5.2 **Sedimentation.**

Sedimentation can be defined as the falling of a suspension of particles in a stationary fluid. The swarm particles has a velocity $u_v(\varepsilon)$ and all the particles in the swarm have the same velocity equal to the swarm velocity. The interstitial fluid velocity is equal to the amount of fluid displaced by the particles as a function of time, divided by the open area between the particles.

Now for a system during sedimentation on the following equations can be defined:

$$u = 0$$
$$u_v(\varepsilon) = v_d \neq 0 \quad \textbf{(1.34)}$$

$$v_i = -\frac{(1-\varepsilon)v_d}{\varepsilon} \quad \textbf{(1.35)}$$

$$v_s = v_d - v_i \quad \textbf{(1.32)}$$

$$v_i = v_d + \frac{(1-\varepsilon)v_d}{\varepsilon} = \frac{v_d}{\varepsilon} \quad \textbf{(1.36)}$$

1.5.3 **Similarity between Fluidization and Sedimentation.**

$u_v(\varepsilon)$ is defined as velocity of a swarm particles, with porosity ε, in absence of a superficial fluid velocity during sedimentation. U is defined as the superficial fluid velocity in order to obtain a porosity ε in a fluidized bed. The drag on a particle in each case is equal to its weight in the liquid, and since the slip velocity, v_s, is a unique function of the physical properties of the liquid, the particle diameter, the distance between the particles and the drag force, v_s must be the same in both cases to obtain a porosity ε.

Fluidization:

$$v_{s1} = -\frac{u}{\varepsilon}$$

Sedimentation:

$$v_{s2} = \frac{v_d}{\varepsilon} = \frac{u_v(\varepsilon)}{\varepsilon} \quad \textbf{(1.37)}$$

$v_{s1} = v_{s2}$ hence:

$$u_v(\varepsilon) = -u$$

Thus the sedimentation velocity of a swarm particles with porosity ε, $u_v(\varepsilon)$, is equal to the superficial fluid velocity, u, necessary to obtain a porosity ε in a fluidized bed [1.2].

1.5.4 **Combination of Fluidization and Sedimentation.**

In a system in which the superficial fluid velocity does not equal the swarm velocity, particles will move in an up- or downwards direction depending on the value of the superficial velocity. The particle velocity is a summons of the superficial fluid velocity and the swarm velocity. And the interstitial fluid velocity is a combination of the displaced fluid

by the moving particles and the influence of the superficial fluid velocity. For a combined system the following velocities can be defined:

$$u_v(\varepsilon) \neq v_d \neq u \neq 0 \qquad \textbf{(1.38)}$$

$$v_d = u + u_v(\varepsilon) \qquad \textbf{(1.39)}$$

$$v_i = -\frac{(1-\varepsilon)v_d}{\varepsilon} + \frac{u}{\varepsilon} \qquad \textbf{(1.40)}$$

$$v_s = v_d - v_i \qquad \textbf{(1.32)}$$

$$v_s = \frac{v_d}{\varepsilon} - \frac{u}{\varepsilon} \qquad \textbf{(1.41)}$$

From these equations of the combined system, the equations of a sedimentation or fluidization system can be obtained by using u = 0 or $v_d = 0$.

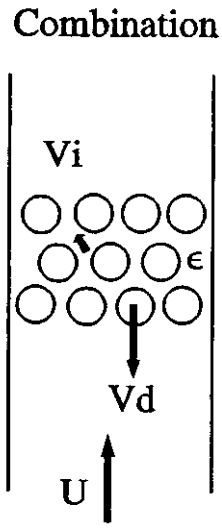

Figure 1.7 Velocities in a combined system.

1.5.5 **Volumetric flux in a combined system.** [1.4]

The symbol J is used to represent total volumetric flux, in meters per second, or volumetric flow rate per unit area. The flux is related to the local component concentration and velocities.
The amount of particles leaving the unit area per second (particle volumetric flow) is given by:

$$J_p = v_d(1-\varepsilon) \qquad \textbf{(1.42)}$$

The amount of fluid leaving the area per second (fluid volumetric flux) is given by:

$$J_f = \varepsilon v_i \tag{1.43}$$

In the literature [1.5,1.6] these fluxes are sometimes defined as the superficial fluid or particle velocities, but J_f is not always the same as the superficial fluid velocity "u" defined in the previous paragraph. In a fluidized system J_f is equal to "u" because $v_i = u/\varepsilon$, but in a combined system $v_i = -(1-\varepsilon)v_d/\varepsilon + u/\varepsilon$ hence:

$$J_f = -(1-\varepsilon)v_d + u \tag{1.44}$$

The total local flux is given by:

$$J = J_f + J_p$$

$$J = v_d(1-\varepsilon) + \varepsilon v_i \tag{1.45}$$

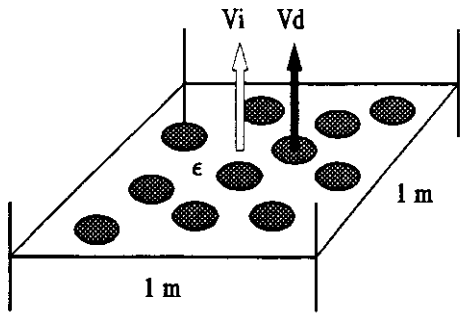

Figure 1.8 Volumetric flow per unit

The slip velocity is defined as the particle velocity minus the interstitial fluid velocity, $v_p - v_i$, so combining equation (1.41) and equation (1.42) gives:

$$v_s = v_d - v_i$$

$$v_s = \frac{J_p}{1-\varepsilon} - \frac{J_f}{\varepsilon} \tag{1.46}$$

Drift velocities are defined as the difference between the component velocity and the average as follows:

$$v_{dj} = v_d - J$$

$$v_{fj} = v_i - J \tag{1.47}$$

where ν_{dj} = particle drift velocity and ν_{fj} = fluid drift velocity.

The **drift flux** represents the volumetric flux of a component relative to a surface moving at the average velocity:

$$J_{df} = (1-\varepsilon)(\nu_d - J)$$
$$J_{fd} = \varepsilon(\nu_i - J) \qquad \textbf{(1.48)}$$

where J_{df} = particle drift flux and J_{fd} = fluid drift flux.
It can be proven that $J_{df} = -J_{fd}$

Combining equations (1.41), (1.44) and (1.45) gives:

$$J_{df} = \varepsilon(1-\varepsilon)\nu_s \qquad \textbf{(1.49)}$$

Therefore the drift flux is proportional to the relative velocity.

Using equation (1.40) for v_s gives for the drift flux:

$$J_{df} = \varepsilon(1-\varepsilon)\left(\frac{\nu_d}{\varepsilon} - \frac{u}{\varepsilon}\right) \qquad \textbf{(1.50)}$$

Now it is possible to calculate the drift flux for a fluidized system an hindered settling system and a combined system.

References:

[1.1] Stokes, G.G
Mathematical and physical papers
Trans. Cambridge Phil. Soc. 9, part II, 51ff, 1851

[1.2] Richardson J.F., Zaki W.N.
Sedimentation and Fluidization: Part I
Trans.Inst.Chem.Engrs, Vol. 32, 1954.

[1.3] Richardson, J.F. and Meikle, R.A.
Sedimentation and fluidization, part 3
Trans. Inst. Chem. Eng., 39, 348-356, 1961

[1.4] Concha F, Almendra E.R.
Settling velocities of particulate systems, 2. settling velocities of suspensions of spherical particles.
International Journal of Mineral Processing, 6 (1979) 31-41.

[1.5] Wallis G.B.
One-dimensional two-phase flow.
McGraw-Hill Book Company, New York. 1969.

[1.6] Wallis G.B.
A simplified one-dimensional representation of two-component vertical flow and its application to batch sedimentation
Symposium on the interaction between fluids and particles. London 20-22 june 1962.

CHAPTER 2. Sedimentation.

The previous chapter dealt with forces, acting on an isolated particle, moving relative to a fluid, and it was shown that the frictional drag can be expressed in terms of a friction factor f, which was a function of the particle Reynolds number.
If the particle is settling in a gravitational field, it quickly reaches it terminal falling velocity when the frictional force has become equal to the net gravitational force.
In practice, the concentration of particles in suspension will be high enough for there to be significant interaction between the particles, and the frictional force exerted at a given velocity of the particles relative to the fluid may be greatly increased as hindered settling takes place.
As a result, the sedimentation rate of a particle in a suspension may be considerably less than its terminal falling velocity under free settling conditions when the effect of mutual interference is negligible.
In this chapter, the behaviour of concentrated suspensions will be discussed and the equipment for concentrating or thickening such suspensions will be reviewed.
It should be noticed that suspension of fine particles behave rather differently from coarse suspensions, in that a high degree of flocculation may occur as a result of the very high specific surface of the particles. Therefore, fine and coarse suspensions will be treated separately.
Sedimentation is an important operation, e.g. in the purification of waste water, the thickening of concentrates and tailings with a return of water into the circuit and the separation of leach liquor and ore in hydrometallurgy.
This chapter will discuss the calculation method for the equipment to be used on the basis of laboratory experiments. These methods are relatively simple for dilute suspensions.
The calculation procedure for thickeners in which a concentrated suspension has to be produced is much more complicated, especially in the case of flocculated materials.
The method developed by Coe and Clevenger [2.1] in 1916 is still the most widely used one, even though one could point out some fundamental shortcomings of this method.
In 1952 the mathematician Kynch [2.2] published an elegant mathematical analysis of the sedimentation process. The purpose of this contribution was to alleviate some of the shortcomings of the Coe and Clevenger method. However, the approach by Kynch is not universally applicable, since this theory is not valid for the compression zone.
At the present time, our knowledge of the behaviour of a suspension in this zone is rather limited, hence liberal use is made of safety factors to overcome the shortcomings.

2.1 *Fine suspensions.*

In 1916, Coe and Clevenger [2.1] published an article, pointing out that a concentrated suspension may settle in two different ways.
At first, after an initial brief acceleration period, the interface between the clear liquid and the suspension moves downwards at a constant rate and a layer of sediment builds up at the bottom of the basin. When this interface approaches the layer of sediment, its falling rate will decrease until the 'critical settling point' is reached when a direct interface is formed between the sediment and the clear liquid. Further sedimentation then only takes place because of a consolidation of the sediment, with liquid being forced upwards around solids which are then

forming a loose bed with the particles in contact with one another. Since the flow area is gradually being reduced, the rate progressively diminishes.

In Figure 2.1, the sedimentation process is illustrated. A is clear liquid, B is suspension of the original concentration, C is a layer through which the concentration gradually increases, and D is sediment.
The sedimentation rate remains constant until the upper interface corresponds with the top of zone C and it then falls until the critical settling point is reached when both zones B and C will have disappeared.
The main reasons for the change in settling rate of the particles in a concentrated suspension are as follows:
(i) The large particles are settling relative to a suspension of smaller ones, so that the effective density and viscosity of the fluid are increased.
(ii) The upward velocity of the fluid displaced during settling is appreciable in concentrated suspensions and the apparent settling velocity is less than the actual velocity relative to the fluid.
(iii) The velocity gradients in the fluid close to the particles are increased as a result of the change in the area and shape of the flow spaces.
(iv) The smaller particles tend to be dragged downward by the motion of the large particles and therefore accelerated.
(v) Because the particles are closer together in a concentrated suspension, flocculation is more marked in an ionized solvent and the effective size of the small particles is increased.

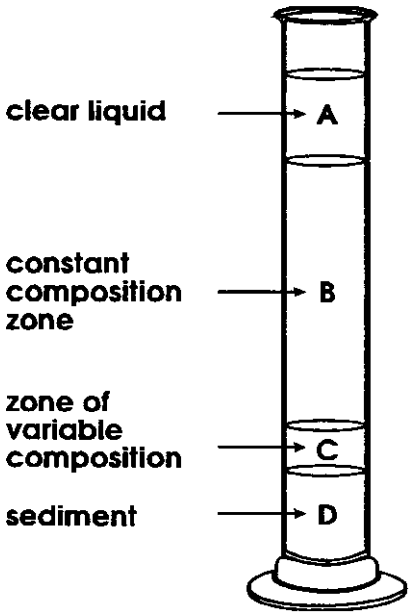

Figure 2.1 Sedimentation of concentrated suspensions.

If the range of particle size is not more than about 6:1, a concentrated suspension settles with a sharp interface and all the particles fall at the same velocity. This is in contrast with the behaviour of a single particle in a dilute suspension, for which the settling velocity is greater for larger particles. The overall result is that in a concentrated suspension the large particles are retarded and the small particles accelerated.
A number of attempts have been made to predict the apparent settling velocity in a concentrated suspension. Even though several different types of empirical equations have

been suggested, they are all a modification of equation (1.12), by replacing the fluid properties by the suspension (subscript c) properties:

$$v_f = \frac{1}{18}\frac{d^2(\rho_s - \rho_c)g}{\mu_c} \qquad \textbf{(2.1)}$$

where

$$\rho_s - \rho_c = \varepsilon(\rho_s - \rho_f) \qquad \textbf{(2.2)}$$

and

$$\mu_c = \mu(1 + k\Phi) \qquad \textbf{(2.3)}$$

ν_f is the sedimentation velocity of a particle, d is the particle diameter, ρ is the density, μ the viscosity and g the gravity acceleration. k is a constant (2.5 for spheres) and Φ is the volumetric concentration of the particles, ε is the voidage of the suspension.
In some other cases, equation (1.12) was simply modified by multiplying the right hand side by a correction factor f(ε):

$$f(\varepsilon) = \varepsilon^2 \cdot 10^{-1.82(1-\varepsilon)} \qquad \textbf{(2.4)}$$

Generally, the rate of sedimentation of a suspension of fine particles is difficult to predict because of the large number of factors involved, such as the presence of an ionized solution, the degree of agitation, and so forth.
The higher the concentration of suspension, the lower the falling rate of the sludge line because the greater is the upward velocity of the displaced fluid and the steeper are the velocity gradients in the fluid. Figure 2.2 shows the settling curves for the sedimentation of calcium carbonate in water; Figure 2.3 shows the mass rate of sedimentation versus the concentration.

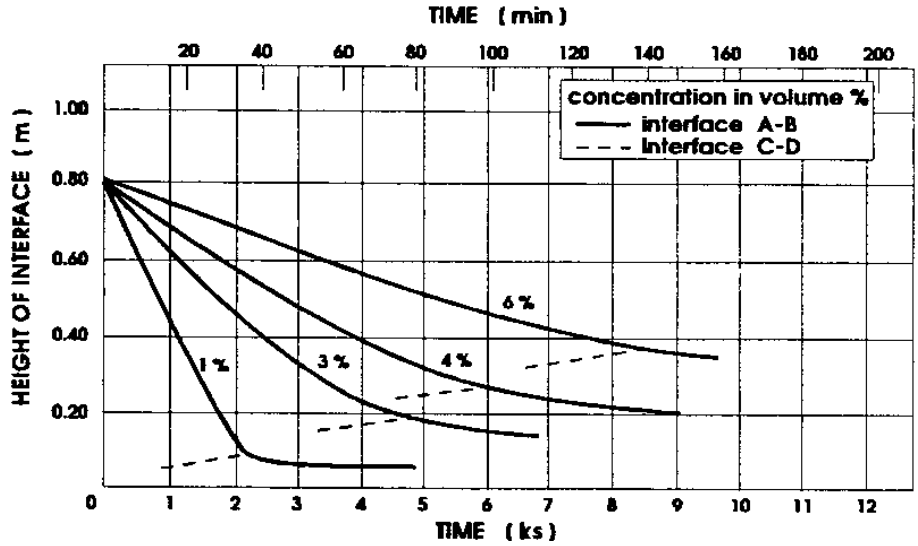

Figure 2.2 Effect of concentration on sedimentation of $CaCO_3$

Figure 2.3 shows a maximum, followed by a gradual decrease. The final consolidation of the sediment is the slowest part of the process because the displaced fluid has to flow through the small spaces between the particles. As consolidation occurs, the rate falls off because the resistance to the flow of liquid progressively increases. The porosity of the sediment is smallest at the bottom, because the compressive force due to the weight of the particles is greatest and because the lower portion was formed at an early stage in the sedimentation process.

The rate of sedimentation during this period according to Roberts [4.3] can be given by:

$$-\frac{dH}{dt} = k(H - H_\infty) \tag{2.5}$$

where H = the height of the sediment at time t
H_∞ = final height of the sediment
k = constant for a given suspension

or

$$\ln(H - H_\infty) = -kt + \ln(H_0 - H_\infty) \tag{2.6}$$

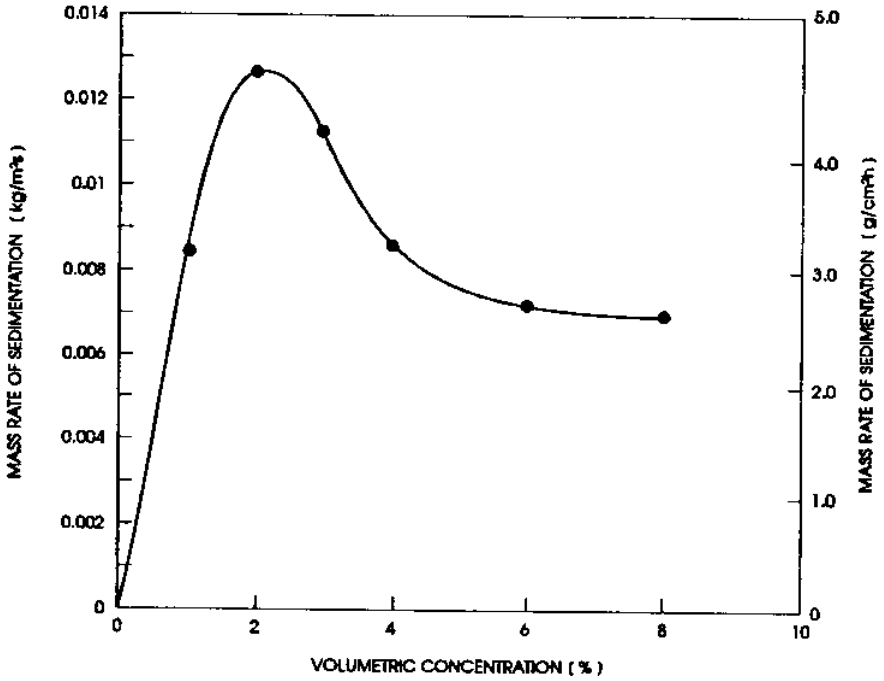

Figure 2.3 Concentration on mass rate of sedimentation

If $\ln(H-H_\infty)$ is plotted against time, there will be a discontinuity at the point of entrance of the compression zone at $t=t_c$. (See Figure 2.4)

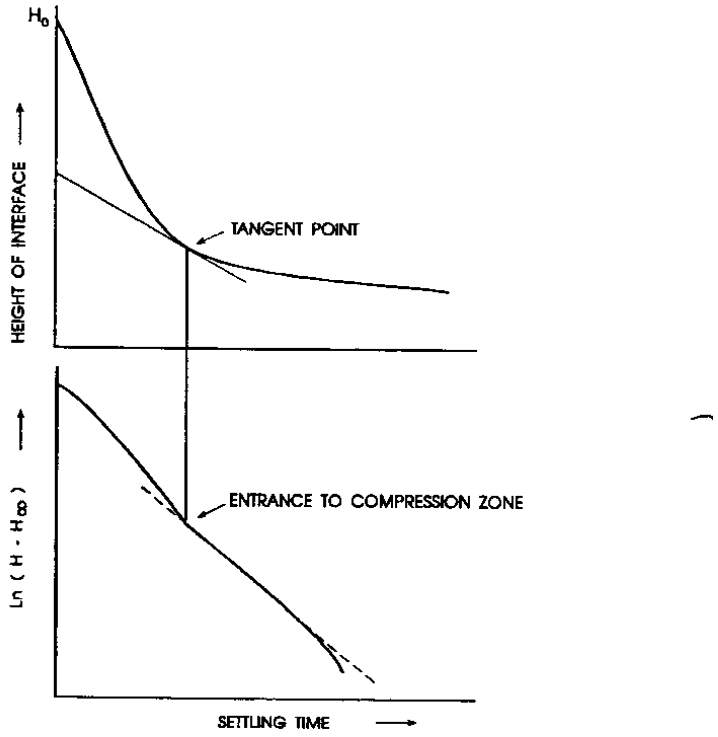

Figure 2.4 Roberts' method for locating the compression point

The slope of the tangent at $t=t_c$ at the settling curve represents the settling velocity.

Coe and Clevenger presented the first truly successful method for the estimation of thickener area requirements using batch settling curves. The area A is given by:

$$A = \text{overflow rate} \ / \ \text{settling rate} \tag{2.7}$$

The overflow rate refers to the volume of liquid which remains to be disengaged from the solids as it settles at various concentrations between the feed and the underflow. Coe and Clevenger further assumed that the settling rate is a function of local solids concentration only. It is customary to refer to the unit area requirement A of a suspension. This is defined as the area required to settle a slurry with a steady feed rate of 1 ton of dry solids per 24 hours. On this basis equation (2.7) may be rewritten as:

$$A = \frac{K(D_i - D_u)}{\nu} \tag{2.8}$$

where
- K = Coe and Clevenger constant, $1/\rho_L$
- ρ_L = liquid density
- D_i = initial dilution, mass of water per mass of solids
- D_u = final dilution
- ν = settling rate

A series of settling tests is conducted at different solutions ranging from that of feed to that of the underflow. For each dilution A is calculated from equation (2.8) using the initial settling rate. The maximum value of A is used for design.

2.2 *Coarse suspensions*

Richardson and Zaki [2.2] have studied the falling velocity of coarse suspensions and found the following relationship for velocities in such a system (see also chapter 1, eqn (1.19)):

$$\frac{\nu_f}{\nu_0} = \varepsilon^n \tag{2.9}$$

where ν_f = falling velocity of the suspension and ν_0 = terminal falling velocity of the particle. Not all authors represent their findings in a similar manner, there are about as many suggested relationships as there are authors. Also for the value of the coefficient n in equation (2.6), many relationships exist, it is therefore suggested to use equation (1.20) which gives a reasonable approximation of a large number of equations.

2.3 *Solid flux in batch sedimentation*

In a sedimenting suspension, the sedimentation velocity v_f is a function of the concentration C and the mass rate of sedimentation per unit area or flux ψ is equal to the product Cv_f. Thus:

$$\psi = Cv_f = v_f(1-\varepsilon)\rho_s \qquad \textbf{(2.10)}$$

Together with equation (2.9), this equation can be rewritten as:

$$\psi = v_0\varepsilon^n(1-\varepsilon)\rho_s \qquad \textbf{(2.11)}$$

From the form of the function, it can be seen that ψ should have a maximum between 0 and 1. It can be derived that:

$$\frac{d\psi}{d\varepsilon} = v_0\rho_s[n\varepsilon^{n-1}(1-\varepsilon)-\varepsilon^n] = v_0\rho_s[n\varepsilon^{n-1}-(n+1)\varepsilon^n] \qquad \textbf{(2.12)}$$

When $d\psi/d\varepsilon=0$, then:

$$n\varepsilon^{n-1}(1-\varepsilon)-\varepsilon^n = 0 \qquad \textbf{(2.13)}$$

or

$$\varepsilon = \frac{n}{1+n} \qquad \textbf{(2.14)}$$

If n ranges from 2.4 to 2.6 as for suspensions of uniform spheres, the maximum flux should occur at a voidage between 0.71 and 0.82 (volumetric concentration 0.29 to 0.18).
Similarly, it can be derived that at the point of inflexion ($d\psi^2/d\varepsilon^2 = 0$):

$$\varepsilon = \frac{n-1}{n+1} \qquad \textbf{(2.15)}$$

which corresponds with a voidage ε between 0.41 and 0.65, corresponding to high concentrations (C=0.59 to 0.35)

It should be noted that the point of inflexion occurs at a value of the voidage ε below that at which the mass rate of sedimentation ψ is a maximum. For coarse particles (n=2.4), the point of inflexion is not of practical interest, since the concentrations at which it occurs (c=0.59) corresponds to a packed bed rather than a suspension.
Figure 2.5 shows the variation of the flux ψ with voidage ε and volumetric concentration C for a value of n=4.6.

***2.4** Kynch analysis of sedimentation*

The mathematician Kynch [2.3] has made an elegant analysis of batch or unsteady state settling by making the following assumptions:

- the particle concentration is uniform across a horizontal layer
- there is no difference in settling due to differences in shape, size or composition
- the sedimentation velocity of the particles depends only on the local concentration

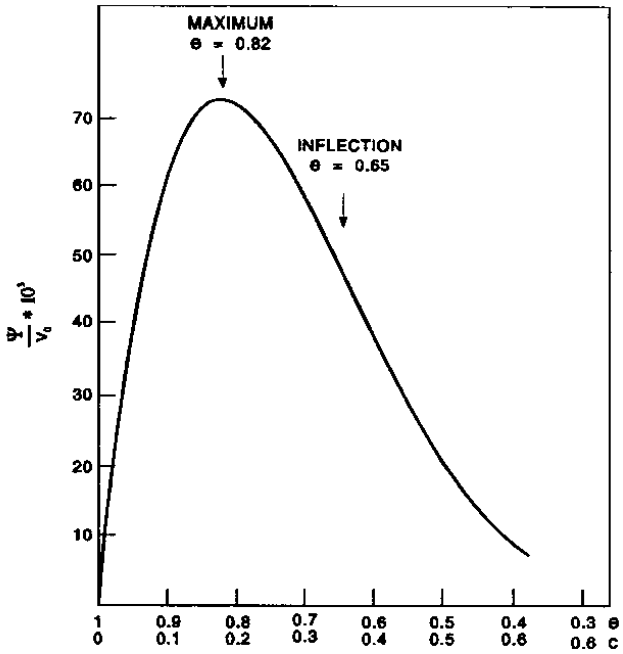

Figure 2.5 Flux-concentration curve for a suspension with n=4.6.

In a batch test starting at uniform concentration, all the solids start settling at uniform velocity ν, since ν=f(C). As the settling solids begin to collapse against the bottom of the sedimentation tank, they must pass through all concentrations between starting concentration and that of the deposited solids. If, at any of these intermediate concentrations, the solidshandling capacity is less than that of the lower concentration immediately above it in the tank, a zone of such intermediate concentration must build up, since the solids cannot pass through it as fast as they are settling down into it.
Kynch showed that the rate of upward propagation of each such constant concentration zone is constant.
Consider the infinitely thin layer at the upper boundary of such a zone, having concentration C, originating at the bottom and moving upward at a velocity u. The solids settling into this layer come from a layer having a concentration (C-dC) and a settling velocity with respect to the tank of (ν-dν) but with respect to the local layer of (ν+dν+u). The concentration of solids settling out of this layer will be C with a settling velocity of ν with respect to the tank and (ν+u) with respect to the layer. Since the concentration of the layer is constant, the quantity

of solids settling into the layer must be equal the quantity of solids settling out of the layer and the materials balance is therefore:

$$(C - dC)A(v - dv + u) = CA(v + u)$$

(2.16)

where A is the thickener area. By solving for u and deleting second order terms:

$$u = -C\frac{dv}{dc} - v$$

(2.17)

Since ν=f(C), it follows that

$$\frac{dv}{dC} = f'(C)$$

(2.18)

hence

$$u = Cf'(C) - f(C)$$

(2.19)

Since C is constant for the layer in question, f(C) and f'(C) have fixed values and therefore u must also be constant.

The constancy of u may be used to calculate the concentration of the sedimentation layer - liquid interface at any time. Let C_0 and H_0 be the initial concentration and height, respectively, of a column of particles in batch settling test. The total weight of solids is C_0H_0A. When any capacity limiting concentration layer reaches the sediment - liquid interface, all solids on the bottom must have passed through it, since it was propagated up from the bottom. If the concentration of this layer is C_2 and it reaches the interface at time t_2, then the quantity of solids having passed through this layer $C_2At_2(\nu_2+u_2)$ must equal the total weight of solids in the column. Equating these expressions gives:

$$C_0H_0A = C_2At_2(v_2 + u_2)$$

(2.20)

If H_2 represents the height of the interface at time t_2, and since the upward velocity of any specific layer is constant:

$$u_2 = \frac{H_2}{t_2}$$

(2.21)

Substituting equation (2.21) into equation (2.20) gives:

$$C_2 = \frac{C_0 H_0}{H_2 + \nu_2 t_2}$$

(2.22)

ν_2 is equal to dH/dt at the point on the setting curve (Figure 2.6) at which the layer having a concentration of C_2 comes to the surface of the sediment. ν_2 is the slope of the tangent to the curve at H_2, t_2). The tangent intercepts the ordinate at H_i. The slope of this line is:

$$\frac{H_i - H_2}{t_2} = \nu_2$$

(2.23)

Combining equations (2.23) en (2.22) yields:

$$C_2 = \frac{H_0}{H_i} C_0$$

(2.24)

It follows that H_i is the height which the slurry would occupy if all the solids present were at concentration C_2. For any arbitrarily chosen value of C_2 the corresponding value of H_i may be calculated. ν_2 can then be determined as the slope of the line drawn through H_i and tangent through the settling curve, and a complete set of data showing ν as f(C) can therefore be developed from one settling test.
The various values of ν and the corresponding values of C can be substituted in the Coe and Clevenger formula for unit area. The concentration layer which gives the largest unit area is then used as the design basis.

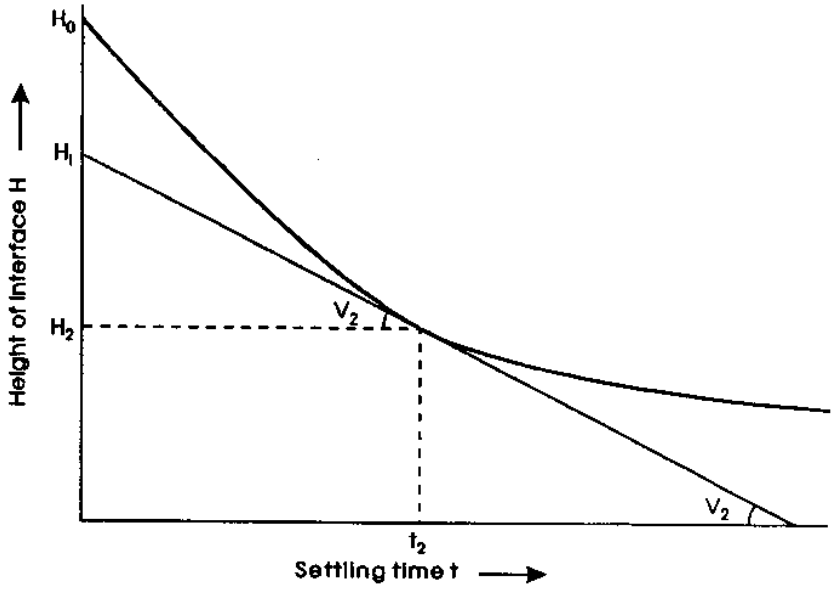

Figure 2.6 Kynch construction

2.5 *Thickener operation*

A thickener is an industrial piece of equipment in which the concentration of a suspension is increased by sedimentation. Usually the concentration of the suspension is high and hindered settling takes place.
The thickener usually consists of a cylindrical tank with a slightly conical bottom. The slurry is fed at the centre, the concentrated slurry is removed from the bottom and the overflow is clarified liquid. Good operation of a thickener requires the existence of a zone of negligible solid contents near the top. In this zone conditions approach those under which free settling takes place. If this zone is too shallow, smaller particles may escape in the liquid overflow. The volumetric upward flow rate of the liquid through the clarification zone is equal to the difference between the feed rate of the slurry and the removal rate in the underflow. Thus the concentration of the solids in the underflow, as well as the throughput, determines the conditions in the clarification zone.
In a continuous sedimentation tank, therefore, one must take into account the downward velocity ν_r, arising from the removal of the underflow.
If the area of the settling zone in the thickener is A, then the volumetric rate of sedimentation q is given by:

$$q = (\nu_f + \nu_r)AC \tag{2.25}$$

where ν_f is the sedimentation velocity at a concentration C in a batch system.
In the underflow, the corresponding equation is:

$$q = (\nu_b + \nu_r)AC_b \tag{2.26}$$

where C_b is the concentration in the underflow and ν_r the sedimentation velocity at a concentration C_b in a batch system.
Equation (2.27) can be rewritten as:

$$\nu_r = \frac{q}{AC_b} - \nu_b \tag{2.27}$$

Substituting this equation in equation (2.25) gives:

$$\frac{q}{A} = \frac{\nu_f - \nu_b}{(1/C) - (1/C_b)} \tag{2.28}$$

In a sedimentation tank, the underflow is small compared to the flow in the settling zone, hence:

$$\frac{q}{A} = \frac{\nu_f C}{1 - (C/C_b)} \tag{2.29}$$

If a suspension of concentration C is fed to the tank at a volumetric rate Q, then

$$\text{rate of solids addition} = QC = \frac{A\nu_f C}{1-(C/C_b)} \quad \textbf{(2.30)}$$

Thus:

$$\frac{C}{C_b} = 1 - \frac{A\nu_f}{Q} \quad \textbf{(2.31)}$$

The area required in the thickener for clarification is then:

$$A = \frac{Q}{\nu_f}(1 - \frac{C}{C_b}) \quad \textbf{(2.32)}$$

This equation can be rearranged somewhat when the mass ratio of liquid to solids in the feed (M_{rf}) and the corresponding value in the underflow (M_{rb}) are used:

$$M_{rf} = \frac{1-C}{C}\frac{\rho}{\rho_s} \wedge M_{rb} = \frac{1-C_b}{C_b}\frac{\rho}{\rho_s} \quad \textbf{(2.33)}$$

Combination with equation (2.33) gives then

$$A = \frac{Q(M_{rf} - M_{rb})C\rho_s}{\nu_f \rho} \quad \textbf{(2.34)}$$

The values of A should be calculated for the whole range of concentrations present in the thickener, and the design should be based on the maximum value obtained.

Example 2.1. [2.5].

A slurry containing 5 kg of water per kg of solids has to be thickened to a slurry containing 1.5 kg of water per kg of solids in a continuous operation. Batch tests yielded the following data:

concentration M_{rf} (kg water/kg solid)	5.0	4.2	3.7	3.1	2.5
rate of sedimentation (mm/sec)	0.20	0.12	0.094	0.070	0.050

Calculate the minimum area of a thickener if the mass rate of solids is 1.33 kg/sec.

Solution:

The condition table as shown on the next page can be constructed. The maximum value of $(M_{rf} - M_{rb})/v = 2.34 \times 10^4$ s/m. Hence from equation (2.35) taking $QC\rho_s = 1.33$ kg/s and taking $\rho = 1000$ kg/m^3, the area becomes:

$$A = 2.34 * 10^4 \frac{1.33}{1000} = 31.2 m^2$$

M_{rf} concentration	$M_{rf} - M_{rb}$ water to overflow	ν_f sedimentation rate, m/sec	$(M_{rf} - M_{rb})/\nu_f$ (sec/m)
5.0	3.5	$2.00*10^{-4}$	$1.75*10^4$
4.2	2.7	$1.20*10^{-4}$	$2.25*10^4$
3.7	2.2	$0.94*10^{-4}$	$2.34*10^4$
3.1	1.6	$0.70*10^{-4}$	$2.29*10^4$
2.5	1.0	$0.50*10^{-4}$	$2.00*10^4$

Example 2.2.

Calculate the minimum area and diameter of a thickener with circular basin to treat 0.1 m^3/s of a slurry of solids concentration 150 kg/m^3. The solids density is 2500 kg/m^3, the liquid density 100 kg/m^3. The results of batch settling tests were as follows:

solids concentration kg/m^3	settling velocity m/s
100	$1.48*10^{-4}$
200	$0.91*10^{-4}$
300	$0.55*10^{-4}$
400	$0.33*10^{-4}$
500	$0.21*10^{-4}$
600	$0.15*10^{-4}$
700	$0.10*10^{-4}$
800	$0.07*10^{-4}$

900	$0.06*10^{-4}$
1000	$0.04*10^{-4}$
1100	$0.03*10^{-4}$

A value of 1290 kg/m^3 for underflow concentration was selected from a retention time test. Estimate the underflow volumetric flow rate assuming total separation of all solids and a clear overflow.

Solution:

At a solids concentration of 100 kg/m^3, 1 m^3 contains 100 kg solids, corresponding with a volume of 100/2500 = 0.04 m^3, hence the water volume is 0.96 m^3 = 960 kg. Then the amount of water per unit weight of solids M_{rf} = 960/100 = 9.6 kg/kg.
At 1290 kg/m^3 the amount of water per unit weight of solids M_{rb} = 0.38 kg/kg. We can now construct the following table:

solids conc. kg/m^3	M_{rf}	sed. rate v_f m/s	$(M_{rf}-M_{rb})/v_f$ s/m
100	9.6	$1.48*10^{-4}$	$6.24*10^4$
200	4.6	$0.91*10^{-4}$	$4.64*10^4$
300	2.9	$0.55*10^{-4}$	$4.62*10^4$
400	2.1	$0.33*10^{-4}$	$5.19*10^4$
500	1.6	$0.21*10^{-4}$	$5.72*10^4$
600	1.3	$0.15*10^{-4}$	$6.15*10^4$
700	1.0	$0.10*10^{-4}$	$6.35*10^4$
800	0.9	$0.07*10^{-4}$	$6.43*10^4$
900	0.7	$0.06*10^{-4}$	$6.04*10^4$
1000	0.6	$0.04*10^{-4}$	$5.35*10^4$
1100	0.5	$0.03*10^{-4}$	$4.09*10^4$

The maximum value of $(m_{rf}-M_{rb})/vf$ = 6.43*104 s/m. The area A can be calculated from equation (2.34). The mass flow rate of solids is $QC\rho_s$ = 0.1*150 = 15 kg/s.
The feed density can be calculated as follows:

> Since the slurry concentration is 150 kg/m^3, 1 m^3 of the slurry contains 150 kg solids which accounts for a volume of 150/2500 = 0.06 m^3. The remaining 0.94 m^3 of water has a mass of 940 kg, hence 1 m^3 has a total mass of (150+940) = 1090 kg, resulting in a feed density of 1090 kg/m^3

hence

$$A = \frac{6.43*10^4*15}{1090} = 885m^2$$

The diameter follows from

$$d = \sqrt{\frac{4A}{\pi}} = \frac{\sqrt{4*885}}{3.14} = 33.6m$$

The volumetric flow rate of the underflow is obtained from a mass balance as

$$Q_b = 0.1*150/1290 = 0.0116m^3/s$$

2.6 *Sedimentation classification.*

The performance of sedimentation classifiers can be developed from the concept of the ideal settling pool. In the ideal pool, the limiting size particles that particle which has a settling rate just sufficient to allow it to settle the depth of the pool during its residency. Particles with higher settling rates will be collected.
The d_{50} or separation size will be that particle which if it enters the pool half way down, just settles to the bottom, since half the particles of this size will initially be lower down and reach the bottom and the other half will be carried out in the overflow. In other words: a particle with size d_{50} has an equal chance of reporting to the underflow or to the overflow.
Extending this concept, it can be seen that the ideal performance curve can be constructed with the relationship:

$$R = \frac{\text{settling rate of particle of size d}}{\text{settling rate of limiting size particle}} \quad \textbf{(2.35)}$$

where R = recovery of d-sized particle in the underflow.
From theoretical diffusion or dispersion models, expressions for R can be derived. In practice, however, the Weibull or Rosin-Rammler relationship is often used:

$$R = 1 - \exp\left[-0.6931\left(\frac{d}{d_{50}}\right)^s\right] \quad \textbf{(2.36)}$$

with s being an empirical parameter in the range 1 .. 3.8.

References:

[2.1] Coe, H.S. and Clevenger, G.H.
Methods for determining the capacities of slime-settling tanks
Trans. Am. Inst. Min. Met. Eng., 55, 1916, 356

[2.2] Kynch, G.J.
A theory of sedimentation
Trans. Faraday Soc. 48, 1052, 166

[2.3] Roberts, M.

Trans AIME, 184, 61, 1949

[2.4] Richardson, J.F. and Zaki, W.N.
Sedimentation and fluidization: Part I
Trans. Instn. Chem. Engrs, Vol.32, 1954

[2.5] Coulson, J.M. and Richardson, J.F.
Chemical Engineering, Volume 2, 3rd Ed.
Pergamon Press, 1978

CHAPTER 3. Fluidization.

If a fluid is passed through a bed of solids, the pressure drop increases as the fluid flow increases and can be calculated using Ergun's formula.
When the frictional drag on the particles becomes equal to their apparent weight (actual weight less buoyancy), the particles become rearranged so that they offer less resistance to the fluid flow, and the bed starts to expand. This process continues as the fluid velocity is increased, until the loosest form of packing is obtained. Now the bed is said to be fully fluidized; further increase of the fluid velocity has little effect on the pressure drop, which remains approximately equal to the weight per unit area of the bed.
Up to this stage the system behaves in a similar way, whether the fluid is a liquid or a gas, but at high velocities there is a clear distinction between the behaviour in the two cases. With a liquid, the bed continues to expand and maintains its uniform character, this type of fluidization is known as particulate or homogeneous fluidization.
With a gas, uniform fluidization only occurs at relatively low fluid velocities. At high velocities two separate phases are formed; the continuous phase or dense phase and the discontinuous or bubble phase. This type of fluidization is called aggregative or heterogeneous fluidization. It has been suggested that the Froude group

$$Fr = \frac{v_{mf}^2}{gd} \qquad \textbf{(3.1)}$$

where v_{mf} = minimum fluid velocity, calculated over the whole cross-section of the bed, at which fluidization takes place
d = diameter of the particles
g = gravity acceleration

At values less than unity, particulate fluidization occurs, at higher values aggregative fluidization takes place.

3.1 *Fluidization velocity and pressure gradient.*

The relation between the superficial velocity v_s of the fluid (calculated over the whole cross-section of the bed) and the pressure drop across the bed is shown in Figure 3.1.
A linear relationship is obtained up to the point where expansion of the bed takes place (A); the slope gradually diminishes as the bed expands. As the velocity is increased, the pressure drop passes through a maximum value (B) and then falls slightly and attains an approximately constant value, independent of the fluid velocity (CD). If the velocity is reduced again, the bed contracts until it reaches the condition where the particles are just resting on one another (E), it then has the maximum stable porosity for a fixed bed. If the velocity is further decreased, the bed remains in this condition provided it is not shaken. The pressure drop (EF) in this fixed bed is then less than the original pressure drop.

The relationship between ΔP and v_s in the fixed bed is given by the Ergun formula. If the flow is laminar, this reduces to the Carman-Kozeny equation in which the relationship between ΔP and v_s is linear.

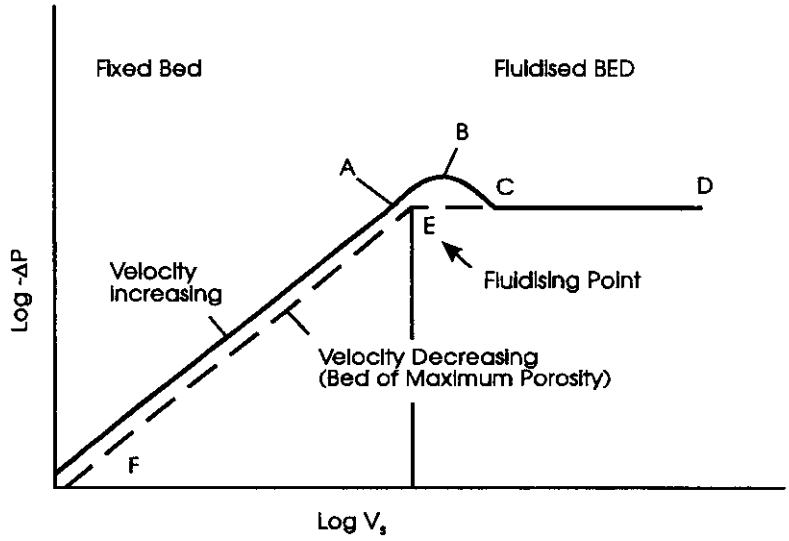

Figure 3.1 Pressure drop across fixed and fluidized beds.

When the fluid velocity has reached a value v_{mp}, ΔP is equal to the apparent weight of the bed and fluidization starts. When the velocity is further increased, the bed expands and the porosity or voidage ε changes until it has reached a maximum value.
In a fluidized bed, the total friction force on the particles must be equal to the effective weight of the bed. Thus in a bed of unit cross sectional area, depth L and porosity ε:

$$\frac{\Delta P}{L} = (1-\varepsilon)(\rho_s - \rho_f)g \qquad \textbf{(3.2)}$$

where ΔP = pressure drop across the bed
g = acceleration due to gravity
ρ_s = solids density
ρ_f = fluid density

For laminar flow, the Carman-Kozeny equation is (see also eqn (1.17)):

$$\frac{\Delta P}{L} = \frac{150(1-\varepsilon)^2 \mu v_s}{\varepsilon^3 d_{vs}^2} \qquad \textbf{(3.3)}$$

where μ = fluid viscosity
d_{vs} = the volume/surface diameter of a particle

The minimum fluidization velocity can now be calculated by combining equations (3.2) and (3.3) for $v_s = v_{mf}$ and $\varepsilon = \varepsilon_{mf}$, which gives:

$$v_{mf} = \frac{d_{vs}^2}{150} \frac{\varepsilon_{mf}^3}{(1-\varepsilon_{mf})} \frac{(\rho_s - \rho_f)g}{\mu}$$

(3.4)

where ε_{mf} = porosity at minimum fluidization.
This is the well-known equation of Leva [3.1]. Values of ε_{mf} will vary considerably, but a typical value is 0.4. Substituting this value gives:

$$v_{mf} = \frac{d_{vs}^2(\rho_s - \rho_f)g}{1406\mu}$$

(3.5)

Example 3.1

Oil with a density of 900 kg/m^3 and viscosity of 0.003 Ns/m^2 passes vertically upward through a bed of catalyst consisting of approximately spherical particles of diameter 0.1 mm and density 2600 kg/m^3. At what mass flow rate per unit area of bed will (I) fluidization, and (ii) transport of particles occur?

Solution:

(I) Assume that laminar flow conditions exist (to be checked later). Equation (3.4) can then be applied with the following data:

$d_{vs} = 10^{-4}$ m
$\rho_s = 2600$ kg/m^3
$\rho_f = 900$ kg/m^3
$g = 9.81$ m/s^2
$\mu = 0.003$ Ns/m^2

As no value for the voidage has been given, ε will be calculated by considering eight close packed spheres of diameter d in a cube of side 2d. Then:

volume of spheres = $8(\pi/6)d^3$
volume of enclosure = $(2d)^3 = 8d^3$

Hence the voidage is $(8d^3-8(\pi/6)d^3)/8d^3=1-(\pi/6)=0.478$. The minimum fluidization velocity becomes:

$$v_{mf} = \frac{(10^{-4})^{-2} * (0.478)^3 * (2600-900) * 9.81}{150 * (1-0.478) * 0.003} = 7.75 * 10^{-5} \text{ m/s}$$

from which the minimum mass flow per unit area follows:

$$G_{mf} = v_{mf}\rho = 7.75 * 10^{-5} * 900 = 0.070 \text{ kg/m}^2 s$$

(ii) Transport of particles will occur when the fluid velocity is equal to the terminal falling velocity of the particles. Using equation (1.12):

$$v_0 = \frac{1}{18}\frac{d^2(\rho_s - \rho_f)g}{\mu}$$
$$= \frac{1}{18}\frac{(10^{-4})^2 * (2600 - 900) * 9.81}{0.003}$$
$$= 0.0031 \text{ m / s}$$

hence the required mass flow is:

$$G = \rho u_0 = 900 * 0.0031 = 2.78 \text{ kg/m}^2\text{s}$$

Check Reynolds number:

$$\text{Re} = \frac{\rho u_0 d}{\mu} = \frac{900 * 0.0031 * 10^{-4}}{0.003} = 0.093$$

from which it can be concluded that the flow region is laminar.

3.2 *Bed expansion.*

It is important to know how the expansion of the bed changes as a function of the fluid velocity v_s. Leva [3.1] based his calculation on:

- the fact that ΔP remains constant
- the application of the Carman-Kozeny equation for the fluidized bed.

The relationship between bed height and porosity is:

$$\frac{L}{L_{mf}} = \frac{1 - \varepsilon_{mf}}{1 - \varepsilon} \qquad \textbf{(3.6)}$$

where L_{mf} = bed height at minimum fluidization velocity.

The Carman-Kozeny equation is written as:

$$\mu v_s L = \frac{\Delta P d_{vs}^2}{150}\left(\frac{(1-\varepsilon)^2}{\varepsilon^3}\right)^{-1} \qquad \textbf{(3.7)}$$

Since ΔP is constant, it follows from equation (3.7) that

$$\mu v_s \frac{L}{L_{mf}} = \text{constant} * \left(\frac{(1-\varepsilon)^2}{\varepsilon^3} \right)^{-1}$$

(3.8)

Experimentally it has been shown that there exists a linear relationship between $\mu\ v_s\ L / L_{mf}$ and $(1-\varepsilon)^2/\varepsilon^3$. For homogeneous fluidization the slope of this relationship is indeed -1.
For heterogeneous fluidization, the slope is -m, where m>1. The value of m depends primarily on the particle size distribution of the bed.
Leva's equation is based on the extrapolation of flow through a particle bed. On the other hand, one could consider a fluid bed as a swarm of particles which is kept in suspension by the fluid. This is the case if the fluidization velocity v_s is equal to the falling velocity of the particles v_f. The latter can be calculated by the equation of Richardson and Zaki [3.2, 3.3]:

$$v_f = v_0 \varepsilon^n$$

(3.9)

where v_0 is the terminal free-falling velocity of a single particle at infinite solution.
The value of n depends on the Reynolds number $Re_p = d_{vs}\ v_s\ \rho_f / \mu$.

$$\begin{aligned} Re_p &< 0.2 && n = 4.65 \\ 0.2 < Re_p &< 1 && n = 4.35\ Re_p^{-0.03} \\ 1 < Re_p &< 500 && n = 4.45\ Re_p^{-0.1} \\ Re_p &> 500 && n = 2.39 \end{aligned}$$

(3.10)

For the calculation of the bed expansion in homogeneous fluidization one can use equation (3.9). Many other relationships exist that can be used in this calculation [3.4].
The method of Leva and Richardson and Zaki are in good agreement and fit the experimental data reasonably well.

3.3 *Viscosity.*

It is difficult to study the rheological behaviour of fluidized beds. One can say that the viscosity is high, in the order of 1 - 10 poise. The particle size distribution of the fluid bed has a major influence on the apparent viscosity. The presence of small particles causes a lubrication effect, lowering the viscosity. This is shown by Matheson et al. [3.5] in Figure 3.2.

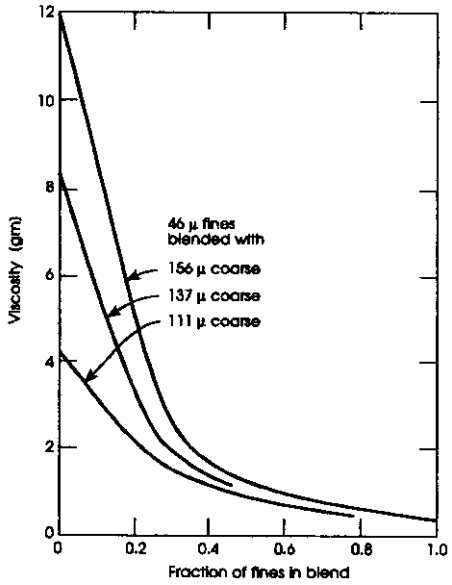

Figure 3.2 Effect of fines on viscosity [3.5].

Trawinski [3.6] proposed the following equation for the apparent viscosity μ^*:

$$\mu^* = \text{constant} * (1 - \varepsilon_{mf}) \rho_f d_{vs} v_s \frac{1}{\Delta L / L_{mf}} \quad \textbf{(3.11)}$$

in which v_s is the superficial velocity, $\Delta L / L_{mf}$ is the bed expansion factor, $\Delta L = L - L_{mf}$ and L_{mf} is the bed height at minimum fluidization.

Figure 3.3 illustrates the findings of different investigators, using particles with different diameters. The results are quite scattered.

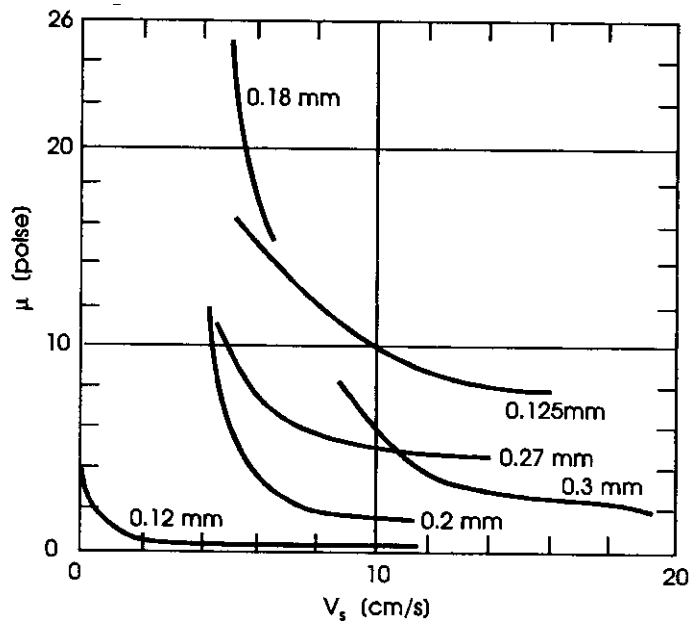

Figure 3.3 Apparent viscosity of gas fluidized beds for different particle sizes

***3.4** Elutriation.*

At high fluid velocities v_s it may happen that particles are blown out of the bed, this is called elutriation. This happens if the value of v_s is much larger than the free falling velocity v_0. Elutriation will have a major impact on the fluidization process and hence it is important to know the relationship between v_0 and the minimum fluidization velocity v_{mf}.
For the free falling velocity of a particle under laminar flow conditions, it was found that (see eqn. (3.12)):

$$v_0 = \frac{1}{18}\frac{d^2(\rho_s - \rho_f)g}{\mu} \qquad \textbf{(3.12)}$$

where v_0 = free falling velocity
d = particle diameter
ρ_s = solids density
ρ_f = fluid density
g = gravity acceleration
μ = viscosity

For the minimum fluidization velocity v_{mf} under laminar flow conditions it was found that

$$v_{mf} = \frac{d^2}{150}\frac{\varepsilon_{mf}^3}{(1-\varepsilon_{mf})}\frac{(\rho_s - \rho_f)g}{\mu} \qquad \textbf{(3.4)}$$

Combination of equation (3.12) and (3.4) gives:

$$\frac{v_{mf}}{v_0} = \frac{18}{50}\frac{\varepsilon_{mf}^3}{(1-\varepsilon_{mf})} \qquad \textbf{(3.13)}$$

For a value $\varepsilon_{mf} = 0.4$ this gives $v_0 \approx 80\ v_{mf}$. Similarly, one can derive that for the turbulent region $v_0 \approx 9\ v_{mf}$.

Example 3.2.

A packed bed consisting of uniform spherical particles (diameter d=3mm, density ρ_s=4200 kg/m^3) is fluidized by means of a liquid. (viscosity μ=0.001 Ns/m^2, density ρ_f=1100 kg/m^3). The voidage of the bed at minimum fluidization is ε=0.48.
Using a modified Ergun equation for the pressure drop through the bed, calculate he minimum fluidizing velocity in terms of the settling velocity v_0 of the particles in the bed. (see also equations (1.15) en (3.3).
The modified Ergun equation for this example is given by:

$$\frac{\Delta P}{L} = \frac{200(1-\varepsilon)^2 \mu v_s}{\varepsilon^3 d^2} + \frac{3.0(1-\varepsilon)\rho v_s^2}{\varepsilon^3 d}$$

Solution:

Using $v_s = v_{mf}$, combination of this modified Ergun equation with equation (3.2) gives:

$$g(\rho_s - \rho_f) = \frac{200(1-\varepsilon)\mu v_{mf}}{\varepsilon^3 d^2} + \frac{3.0\rho v_{mf}^2}{\varepsilon^3 d}$$

Substituting the known data into this equation results in:

$$(4200-1100)*9.81 = \frac{200*(1-0.48)*0.001*v_{mf}}{(0.48)^3*(3*10^{-3})^2} + \frac{3*1100*v_{mf}^2}{(0.48)^3*3*10^{-3}}$$

from which:

$$3.04 = 10.44 v_{mf} + 995 v^2_{mf}$$

which gives a value of $v_{mf} = 0.05$ m/s.

If Stokes law applies, the terminal falling velocity according to (3.12) is:

$$\begin{aligned} v_0 &= \frac{d^2 g(\rho_s - \rho_f)}{18\mu} \\ &= 3*10^{-3}*9.81*3100/18*10^{-3} \\ &= 15.21 \text{ m/s} \end{aligned}$$

The value of Re is then:

$$\text{Re} = 3*10^{-3}*15.21*100/10^{-3} = 5*10^4$$

which is outside the range of Stokes law. In the turbulent region, we can combine equations (3.7) and (3.10) to give:

$$\begin{aligned} v_0^2 &= \frac{3d(\rho_s - \rho_f)g}{\rho_f} \\ &= 3*3*10^{-3}*9.81*3100/1100 \\ &= 0.25 \end{aligned}$$

which gives a value of $v_0 = 0.5$ m/s.

A check on Re gives:

$$\text{Re} = 3*10^{-3}*0.5*1100/10^{-3} = 1650$$

which is still in the turbulent region (Re > 500).
Hence:

$$\frac{v_0}{v_{mf}} = 0.5 / 0.05 = 10$$

As soon as for a particular bed the superficial velocity $v_s > v_0$, elutriation will take place. Yagi and Aochi [3.7] studied elutriation for batch operations and found that their experiments fitted the following elutriation model:

$$-\frac{dX_s}{dt} = k_e X_s \qquad \textbf{(3.14)}$$

where X_s = fraction of fines leaving the bed and k_e = elutriation constant. The solution of (3.14) is:

$$X_s = X_{s0} e^{-k_e t} \qquad \textbf{(3.15)}$$

hence the relationship between X_s / X_{s0} and time is a first order relationship, which is shown in Figure 3.4. X_{s0} is the fraction of fines originally in the bed at t=0.

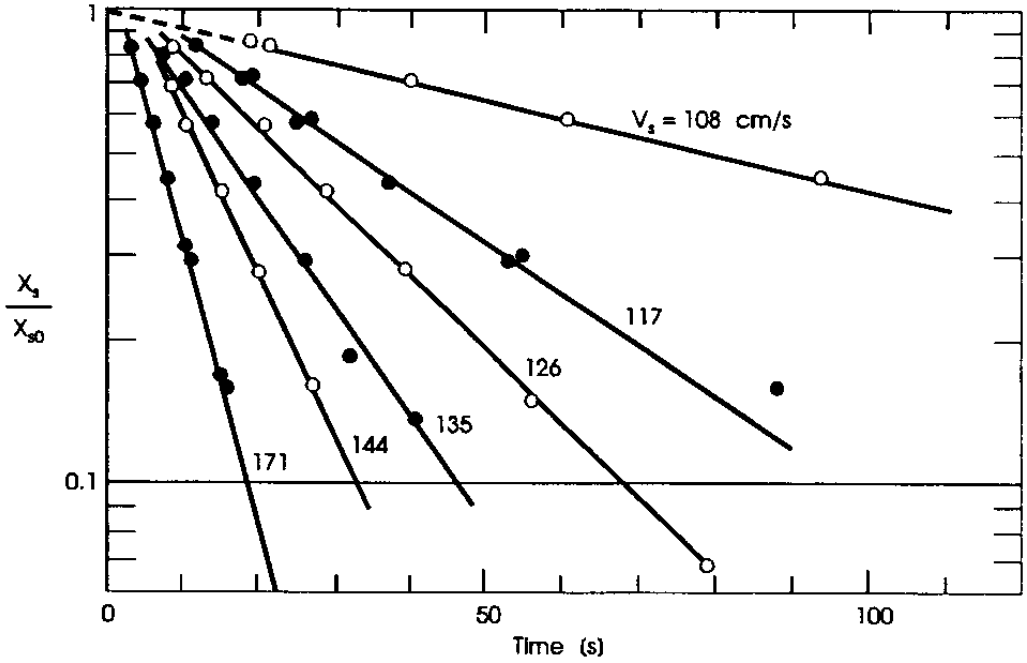

Figure 3.4 Elutriation of glass spheres [3.7].

Figure 3.4 also shows the importance of the influence of the gas velocity on k_e. Leva suggested a relationship of the form:

$$k_e \approx \nu_0^4 \qquad \textbf{(3.16)}$$

For steady state flow experiments, Yagi and Aochi [3.7] correlated the following two groups:

$$\frac{k_e g d_p^2}{\mu(\nu_s - \nu_0)^2} \quad , \quad \frac{\mathrm{d_p} \nu_0 \rho_f}{\mu}$$

as shown in Figure 3.5.

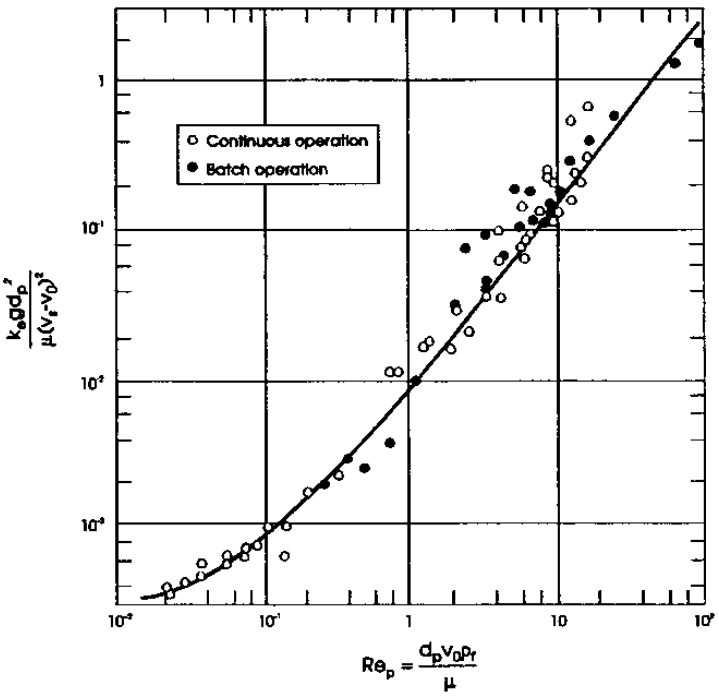

Figure 3.5 Elutriation correlation of Yagi and Aochi. Continuous operation: sand, zinc blende, pyrite cinder, pyrrhotite, calcium carbide, coke. Unsteady operations: sand, glass spheres, iron catalyst, magnesium oxide.

References:

[3.1] Leva, M
Fluidization, Mc Graw-Hill 1959

[3.2] Richardson, J.F. and Zaki, W.N.
Sedimentation and fluidization: Part I
Trans. Instn. Chem. Engrs, Vol. 32, 1954

[3.3] Richardson, J.F. and Meikle, R.A.
Sedimentation and fluidization, Part 3
Trans. Inst. Chem. Engrs., 39, 348-356, 1961

[3.4] Davidson, J.F., Clift, R. and Harrison, D.
Fluidization, Academic Press 1985

[3.5] Matheson, G.L., Herbst, W.A. and Hold, P.A.
Ind. Eng. Chem. 41, 1099, 1948

[3.6] Trawinski, H.
Chem. Ing. Technik, 25, 1953, 229

[3.7] Yagi, S. and Aochi, T.
Paper presented at the Soc. of Chem. Engrs (Japan), Spring Meeting, 1955

CHAPTER 4. Filtration.

Filtration is the removal of solid particles from a fluid, by passing the fluid through a filtering medium on which the solids build up.
The most important factors on which the rate of filtration depends, are:

- the pressure drop across the filter cake and filter medium
- the area of the filtering surface
- the viscosity of the filtrate

Filtration takes place in two operating modes: Constant pressure filtration maintains a constant pressure, the flow rate falls slowly during the cycle. Most continuous filters operate on this principle, the vacuum providing the pressure difference.
Constant rate filtration requires gradually increasing pressure as the cake increases in thickness and hence the resistance to flow increases.
A common approach is to use constant flow rate until the pressure builds up to a certain level and then use constant pressure filtration for the remainder of the time. This can be conveniently achieved using centrifugal pumping.
Continuous filtration in the process industry is usually achieved by using a rotating drum which is partially submerged in the suspension (Figure 4.1). Liquid is drawn through the filter medium, leaving behind a filter cake, which then is also washed and partially dried, before being removed from the filter medium.

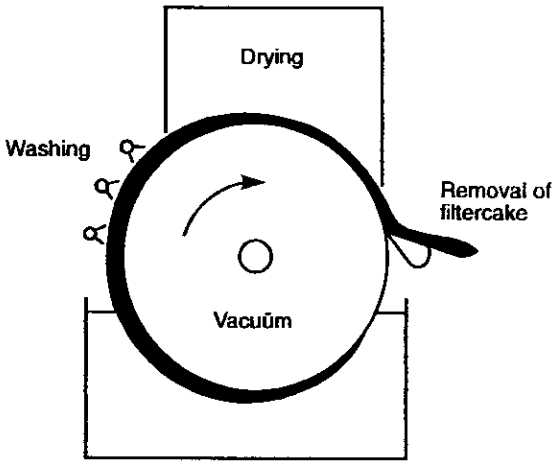

Figure 4.1 Rotating drum filter.

4.1 *Pressure drop through filter cakes.*

Most of the resistance which produces the pressure drop in filtration systems comes from:

- resistance of the filter cake ΔP_c
- resistance of the filter medium ΔP_m

Initially the cake resistance is zero, but as filtration proceeds, it will become the predominant resistance.
There is a similarity between the flow of filtrate through a filter cake and a packed bed. For a packed bed, the Ergun equation (3.14) with laminar flow (Re_p /(1- ε) < 10) reduces to the Carman-Kozeny equation:

$$f = \frac{150(1-\varepsilon)}{\mathrm{Re}_p} \qquad \textbf{(4.1)}$$

where

$$\mathrm{Re}_p = \frac{\rho_f \nu_s d_{vs}}{\mu} \qquad \textbf{(4.2)}$$

and
ρ_f = fluid velocity
ν_s = superficial velocity
μ = fluid viscosity
d_{vs} = the volume/surface diameter of a particle = $6V_p/S_p$
V_p = particle volume
S_p = particle surface area
ε = volume of voids/volume of the bed

In most practical cases, the flow through a filter cake is laminar and the Carman-Kozeny equation can be adapted [4.1, page 128-132]:

$$\frac{\Delta P_c}{\delta_c} = \frac{150(1-\varepsilon)^2 \mu \nu_s}{\varepsilon^3 d_{vs}^2} \qquad \textbf{(4.3)}$$

where
ΔP_c= pressure drop across the cake
δ_c = cake thickness

The cake thickness δ_c can be expressed in terms of the mass of the cake M_c:

$$M_c = \rho_s (1-\varepsilon) A_c \delta_c \qquad \textbf{(4.4)}$$

where
A_c = area of the filter cake
ρ_c = solids density

Combining equations (4.3) and (4.4) results in:

$$\Delta P_c = \alpha \mu \nu_s \frac{M_c}{A_c} \qquad \textbf{(4.5)}$$

with

$$\alpha = \frac{150(1-\varepsilon)}{\varepsilon^3 d_{vs}^2 \rho_s} \qquad \textbf{(4.6)}$$

where α is the specific cake resistance. α is generally not constant for a given system. As the buildup of the cake progresses, ε usually varies.
In most constant pressure filtrations, however, α is fairly constant after an initial period of high flow rate.

The filtration pressure drop ΔP_f must overcome the resistance of the filter medium ΔP_m, which is added to the cake resistance P_c:

$$\Delta P_f = \Delta P_m + \Delta P_c = \mu v_s \left[\frac{\alpha M_c}{A_c} + R_m \right] \qquad \textbf{(4.7)}$$

The superficial velocity v_s can be expressed in terms of V_f, the total volume of filtrate collected:

$$v_s = \frac{dV_f}{dt}\frac{1}{A_c} \qquad \textbf{(4.8)}$$

In addition:

$$M_c = V_f C_c \qquad \textbf{(4.9)}$$

where C_c = the mass of solids deposited as cake per unit volume of filtrate collected.

If the medium resistance Rm is written as:

$$R_m = \frac{\alpha V_e C_c}{A_c} \qquad \textbf{(4.10)}$$

then the filtration equation becomes:

$$\frac{dt}{dV_f} = \frac{\alpha C_c \mu}{A_c^2 \Delta P_f}(V_f + V_e) \qquad \textbf{(4.11)}$$

where V_c = volume of filtrate to build up a fictitious amount of filter cake.

If the slurry is subjected to constant pressure filtration, the graph of reciprocal filtration rate dt/dV_f will have a slope $\alpha C_c \mu / A^2_c \Delta P_f$ and an intercept of

$$\frac{V_e \alpha C_c \mu}{A_c^2 \Delta P_f} = slope * V_e \qquad \textbf{(4.12)}$$

thus allowing α and V_e to be evaluated (see Figure 4.2) for use in equation (4.11).

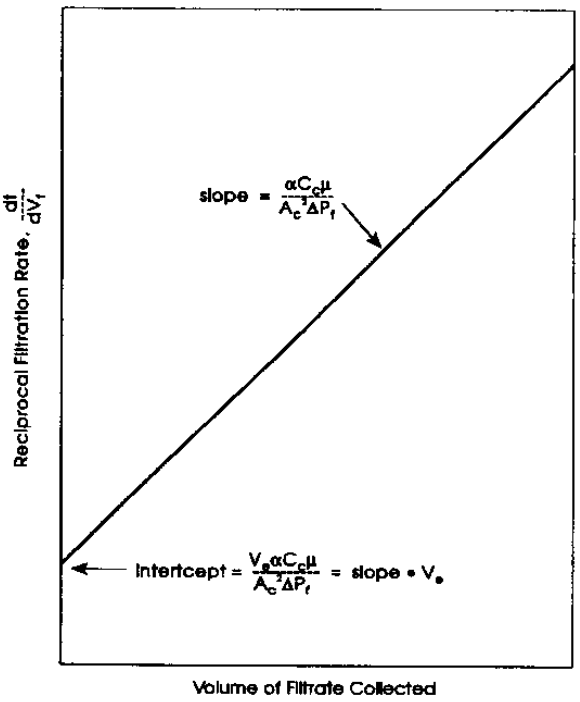

Fig. 4.2 Constant pressure filtration data, evaluation of α and V_e

Since most filter cakes are compressible, α depends on ΔP_f and can be written as:

$$\alpha = \alpha_0 \Delta P_f^n \qquad \textbf{(4.13)}$$

where α_0 and n are empirical constants, n is called the compressibility coefficient and usually has a value between 0.2 and 0.8.

4.2 **Continuous filtration**

In continuous filtration, the pressure drop across the filter is generally kept constant, hence equation (4.11) can be applied and is now written as:

$$\frac{dt}{dV_f} = K_1 V_f + K_2$$

(4.14)

where $K_1 = \alpha C_c \mu / A^2_c \Delta P_f$ and $K_2 = \alpha C_c \mu V_e / A^2_c \Delta P_f$.

Integration of equation (4.13) gives:

$$\int_0^t dt = \int_0^{V_f} (K_1 V_f + K_2) dV_f$$

(4.15)

which results in:

$$t = K_1 \frac{V_f^2}{2} + K_2 V_f$$

(4.16)

Solving this equation for V_f gives:

$$\frac{V_f}{A_c t} = -\frac{K_2}{A_c t K_1} + \left(\frac{K_2^2}{A_c^2 t^2 K_1^2} + \frac{2}{A_c^2 t K_1} \right)^{1/2}$$

(4.17)

When the medium resistance is negligible, equation (4.17) reduces to:

$$\frac{V_f}{A_c t} = \frac{1}{A_c} \left(\frac{2}{K_1 t} \right)^{1/2} = \left(\frac{2 \Delta P_f}{\alpha C_c \mu t} \right)^{1/2}$$

(4.18)

which shows that the filtrate flow rate is inversely proportional to the square root of the specific cake resistance α, the fluid viscosity μ and the cycle time t.

Example 4.1. [4.1]

A slurry containing 0.2 kg of solids (specific gravity 3.0) per kg of water is fed to a rotary drum filter 0.6 m long and 0.6 m diameter. The drum rotates at one revolution in 350 sec and 20 percent of the filtering surface is in contact with the slurry. If filtrate is produced at a rate of 0.125 kg/s and the cake has a voidage of 0.5, what is the thickness of the cake that is produced at a constant pressure drop of 65 kN/m^2. What is the specific cake resistance?

Solution.

Area of the filtering surface = π d l = 0.36π = 1.13 m^2.

The filtrate mass flow is 0.125 kg/s, and since this is the total water flow, the water flow in the feed is also 0.125 kg/s. The solids concentration is 0.2 kg solids/kg water, hence the feed contains:

0.125*0.2 = 0.025 kg solids/s

The volumetric flow of solids becomes then:

$0.025/3000 = 8.33*10^{-6}$ m^3/s

if it would consist entirely out of solids. With a porosity of 50%, however, the volumetric rate of deposition of solids will be twice as high:

$2*8.33*10^{-6} = 1.67*10^{-5}$ m^3/s

Volume of the cake deposited per revolution = $1.67*10^{-5}* 350 = 5.85*10^{-3}$ m^3.

The thickness of the cake produced is therefore:

$5.85*10^{-3}/1.13 = 5.17*10^{-3}= 5.2$ mm

The total volume of filtrate collected $V_f = 1.25*10^{-4}*350 = 4.374*10^{-2}$ m^3.

The filtering surface is submerged for 20 percent of 350 sec = 70 seconds.

The mass of solids deposited per unit volume of filtrate collected is C_c:

$$C_c = \frac{\text{mass of solids}}{\text{volume of filtrate}} = \frac{1.67*10^{-5}*1.5*10^{3}}{1.25*10^{-4}} = 200 kg/m^3$$

Now using equation (4.18) for one revolution of the drum:

$$\alpha = \frac{2\Delta P_f A_c^2 t}{V_f^2 C_c \mu} = \frac{2*65*10^{3}*(1.13)^2*70}{(4.374*10^{-2})^2*200*10^{-3}} = 3.04*10^{10} m/kg$$

Example 4.2.

A plate and frame press, filtering a slurry, gave a total of $8m^3$ of filtrate during the first 1800 s, and another 3 m^3 of filtrate during the next period of 1800 s. What is the final filtration rate? The resistance of the cloth can be neglected and a constant pressure is used throughout.

Solution:

Rewriting equation (4.14) with K2 = 0 and integrating gives:

$$K_1 V_f^2 = 2t$$

When t=1800, Vf=8; when t=3600, Vf=11, hence:

$$K_1[11^2 - 8^2] = 2[3600 - 1800]$$

from which K1 = 63.1.

The constant K2 in equation (4.14) is zero, since the cloth resistance is negligible, hence

$$\frac{dV_f}{dt} = [K_1 V_f]^{-1} = [63.1 * 11]^{-1} = 1.44 * 10^{-3} m^3 / s$$

Example 5.3.

A rotary drum filter of area 3 m^2 operates with an internal pressure of 30 kN/m^2 and with 30% of its surface submerged in the slurry. Calculate the rate production of the filtrate and the thickness of the cake when it rotates at 0.085 Hz (0.5 rev/min), if the filter cake is incomprehensible and the volume of filtrate to build up a fictitious amount of filter cake V_c = $1.3*10^{-4}$ m^3.
The following data is given:

Voidage of cake = 0.4
Specific cake resistance $\alpha = 1.69*10^{-10}$ m/kg
Density of solids = 2000 kg/m^3
Density of filtrate = 1000 kg/m^3
Viscosity of filtrate = 10^{-3} Ns/m^2
Slurry concentration = 20 weight percent solids

Solution:

A 20% slurry contains 20 kg solids per 80 kg solution.
Volume of cake = 20/2000(1-0.4) = 0.0167 m^3.
Volume of liquid in cake = 0.167*0.4 = 0.067 m^3.
Volume of filtrate = (80/1000) - 0.0067 = 0.0733 m^3.
The mass of solids deposited as cake per unit volume filtrate collected C_c = 20/0.0733 = 272 kg/m^3.
The pressure drop $\Delta P = 101.3 - 30 = 71.3*10^3$ N/m^2.
Equation (4.11) can be rewritten to give:

$$\frac{dV_f}{dt} = \frac{A_c^2 \Delta P_f}{\alpha C_c \mu [V_f + V_e]} = \frac{(3)^2 * 71.3 * 10^3}{1.69 * 10^9 * 272 * 10^{-3} * [V_f + 1.3 * 10^{-4}]} = \frac{1.395 * 10^3}{V_f + 0.013}$$

from which

$$V_f^2 / 2 + 0.013 V_f = 1.395 * 10^{-3} t$$

If the speed is 0.083 Hz, one revolution takes 120.5 sec and a given piece of the drum is submerged for 120.5*0.3 = 36.2 s. When t = 36.2 s, V_f may be found by substitution to be 0.303 m^3.

Hence the rate of filtration is 0.303 / 120.5 = 0.0025 m^3/s.
The volume of cake formed per revolution is equal to the volume of cake times the volume of filtrate for one revoluiton per unit volume of filtrate, which gives 0.0167*0.303/0.0733 = 0.07 m^3.
The cake thickness is therefore 0.07/3 = 0.023 m = 23 mm.

4.3 *Washing*

Washing of the cake may be necessary if the filtration liquid is likely to contaminate the cake or if it is too valuable not to recover.
When the washing liquid enters the filter cake, it displaces the pore liquid, initially by plug flow, without dilution. As further washing occurs, the dilution factor increases. This process usually ends when the washing volume is about twice the void volume and the overall removal efficiency rises to 70-90 percent. Further washing has now become very inefficient. Cake wash time is difficult to correlate, but satisfactory results can be obtained in many cases by plotting wash time versus $M_c V_w / A^2_c$ (where M_c = cake mass, V_w = volume of wash liquid), although the linearity tends to fall off after large wash volumes (see Figure 4.3).

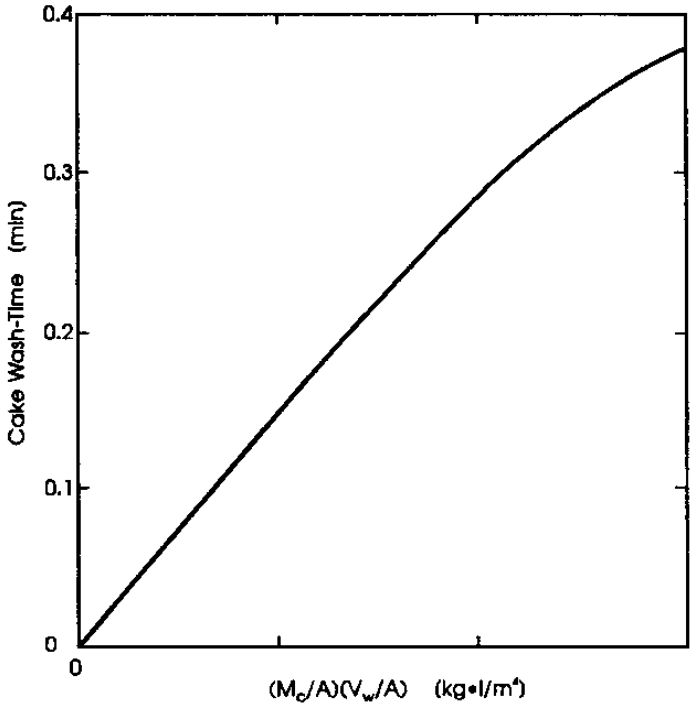

Figure 4.3 Typical cake wash time data.

References:

[4.1] Coulson, J.M., Richardson, J.F.
Chemical Engineering, vol. 2, 3rd Ed., p. 368
Pergamon Press, 1978

CHAPTER 5. Drying.

Drying refers to the removal of liquid from a solid by evaporation. Other methods for separation of the liquid from the solid are not considered drying, such as filtration. In order to separate a liquid from a solid, usually mechanical methods proceed the thermal method, since they are less expensive.
The moisture in a material can be expressed in two ways: dry weight basis expresses the moisture content of wet solids as kilograms of water per kg of dry solid; wet weight basis expresses the moisture in the material as a percentage of the weight of the wet solid. Use of the dry weight basis is recommended, since the percentage change of moisture is constant for all moisture levels. When the wet weight basis is used to express moisture content, a 2 to 3 percent change in the high moisture content (above 75 percent) represents a 15 to 20 percent change in evaporative load. The following relationship holds for the wet and dry weight basis:

$$W_w = \frac{W_d}{1 + W_d}$$

$$W_d = \frac{W_w}{1 - W_w} \qquad \textbf{(5.1)}$$

Where W_w = kg moisture / kg wet solid
W_d = kg moisture / kg dry solid

An excellent overview of drying is given by Perry and Green [5.1], this overview will be closely followed here.

5.1 General conditions for drying.

Solids drying consists of two fundamental and simultaneous processes: (i) heat is transferred to evaporate liquid, and (ii) mass is transferred as a liquid or vapour within the solid and as a vapour from the surface. The factors governing the rates of these processes determine the drying rate.
Commercial dryers differ by the methods of heat transfer employed. Industrial dryers may utilize heat transfer by convection, conduction, radiation, or a combination of these. In each case, however, heat must flow to the outer surface and then into the interior of the solid. Exceptions are microwave drying, radiofrequency drying and drying by Ohmic and inductive heating, in which electricity generates heat internally and produces a high temperature within the material and on its surface.
Mass is transferred in drying as a liquid and vapour within the solid and as vapour from the exposed surfaces. Movement within the solid results from a concentration gradient, which is dependent on the characteristics of the solid. A solid to be dried may be porous or nonporous. It can also be hygroscopic or non-hygroscopic. Many solids fall intermediately between these two extremes, but it is generally convenient to consider the solid to be one or the other.
A study of how a solid dries may be based on the internal mechanism of liquid flow or on the effect of the external conditions such as temperature, humidity air flow, etc., on the drying

rate of the solids. The former procedure generally requires a fundamental study of the internal condition. The latter procedure, although less fundamental, is more generally used because the results have greater immediate application in equipment design and evaluation.

5.2 Internal mechanism of liquid flow.

The structure of the solid determines the mechanism through which internal liquid flow may occur. These mechanisms can include:

(i)	diffusion in continuous, homogeneous solids
(ii)	capillary flow in granular and porous solids
(iii)	flow caused by shrinkage and pressure gradients
(iv)	flow caused by gravity
(v)	flow caused by a vaporization-condensation sequence

In general, one mechanism predominates at any given time during the drying process but it is not uncommon to find different mechanisms predominating at different times during the drying cycle.
The study of internal moisture gradients establishes the particular mechanism which controls the drying process. The experimental determination of reliable moisture gradients is possible by means of MRI.
Hougen, McCauley, and Marshall [5.2] discussed the conditions under which capillary and diffusional flow may be expected in a drying solid and analyzed the published experimental moisture-gradient data for the two cases.

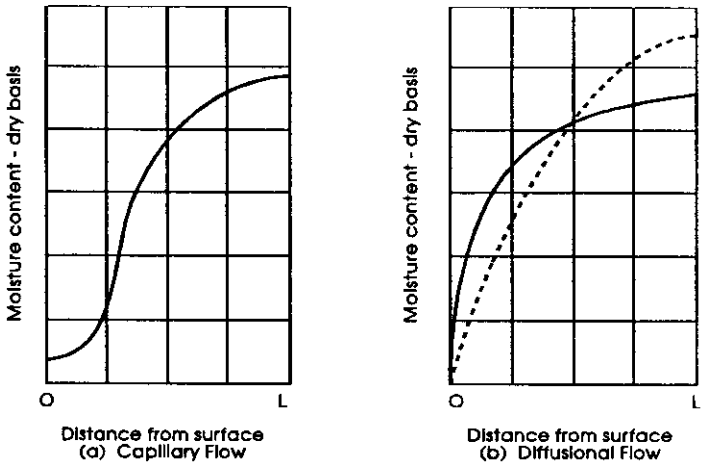

Figure 5.1 Two types of internal moisture gradients in solids drying.

Their curves indicate that capillary flow can be characterized by a moisture gradient involving a double curvature and point of inflection (Fig. 5.1) while diffusional flow is a smooth curve, concave downward (Fig 5.1b), as can be predicted from the diffusion equations. They also showed that the liquid-diffusion coefficient is usually a function of moisture content which decreases with decreasing moisture. The effect of variable diffusivity is illustrated in Fig 5.1b, where the dashed line is calculated for constant diffusivity and the solid line is experimental for the case in which the diffusion coefficient is moisture-

dependent. Thus, the integrated diffusion equations assuming constant diffusivity only approximate the actual behaviour.

These authors classified solids on the basis of capillary and diffusional flow:
Capillary Flow: Moisture which is held in the pores of the solids, as liquid on the surface, or as free moisture in cell cavities moves by gravity and capillarity, provided that channels for continuous flow are present. In drying, liquid flow resulting from capillarity
applies to liquids not held in solution and to all moisture above the fibre-saturation point, as in textiles, paper, and leather, and to all moisture above the equilibrium moisture content at atmospheric saturations, as in fine powders and granular solids, such as paint pigments, minerals, clays, soil, and sand.
Vapour Diffusion: Moisture may move by vapour diffusion through the solid, provided that a temperature gradient is established by heating, thus creating a vapour-pressure gradient. Vaporization and vapour diffusion may occur in any solid in which heating takes place at one surface and drying from the other and in which liquid is isolated between granules of solid.
Liquid Diffusion: The movement of liquids by diffusion in solids is restricted to the equilibrium moisture content below the point of atmospheric saturation and to systems in which moisture and solid are mutually soluble. The first class applies to the last stages in the drying of clays, starches, flour, textiles, paper, and wood, the second class includes the drying of soaps, glues, gelatines, and pastes.
External Conditions: The principal external variables involved in any drying study are temperature, humidity, air flow, state of subdivision of the solid, agitation of the solid, method of supporting the solid, and contact between hot surfaces and wet solid. All these variables will not necessarily occur in one problem.

5.3 *Periods of drying.*

When a solid is dried experimentally, the moisture content (dry basis) W versus time t is as shown in Fig 5.2a. This curve represents the general case when a wet solid loses moisture first by evaporation from a saturated surface on the solid, followed in turn by a period of evaporation from a saturated surface of gradually decreasing area, and, finally, when the latter evaporates in the interior of the solid.
Figure 5.2a indicates that the drying rate is subject to variation with time or moisture content. This variation is better illustrated by graphically or numerically differentiating the curve and plotting dW/dt versus W, as shown in Fig 5.2b, or as dW/dt versus t, as shown in Fig 5.2c. These rate curves illustrate that the drying process is not a smooth, continuous one in which a single mechanism is predominant. Figure 5.2c has the advantage of showing how long each drying period lasts.
The section AB on each curve represents a warming-up period of the solids. Section BC on each curve represents the constant-rate period. Point C, where the constant rate ends and the drying rate begins falling, is called the critical-moisture content. The curved portion CD on Fig. 5.2a is termed the falling-rate period and, as shown in Fig. 5.2b and c, is characterized by a continuously changing rate throughout the remainder of the drying cycle. Point E (Fig. 5.2b) represents the point at which all the exposed surface becomes completely unsaturated and marks the start of that portion of the drying cycle during which the rate of internal moisture movement controls the drying rate Portion CE in Fig. 5.2b is usually defined as the first falling-rate drying period; portion DE, as the second falling-rate period.

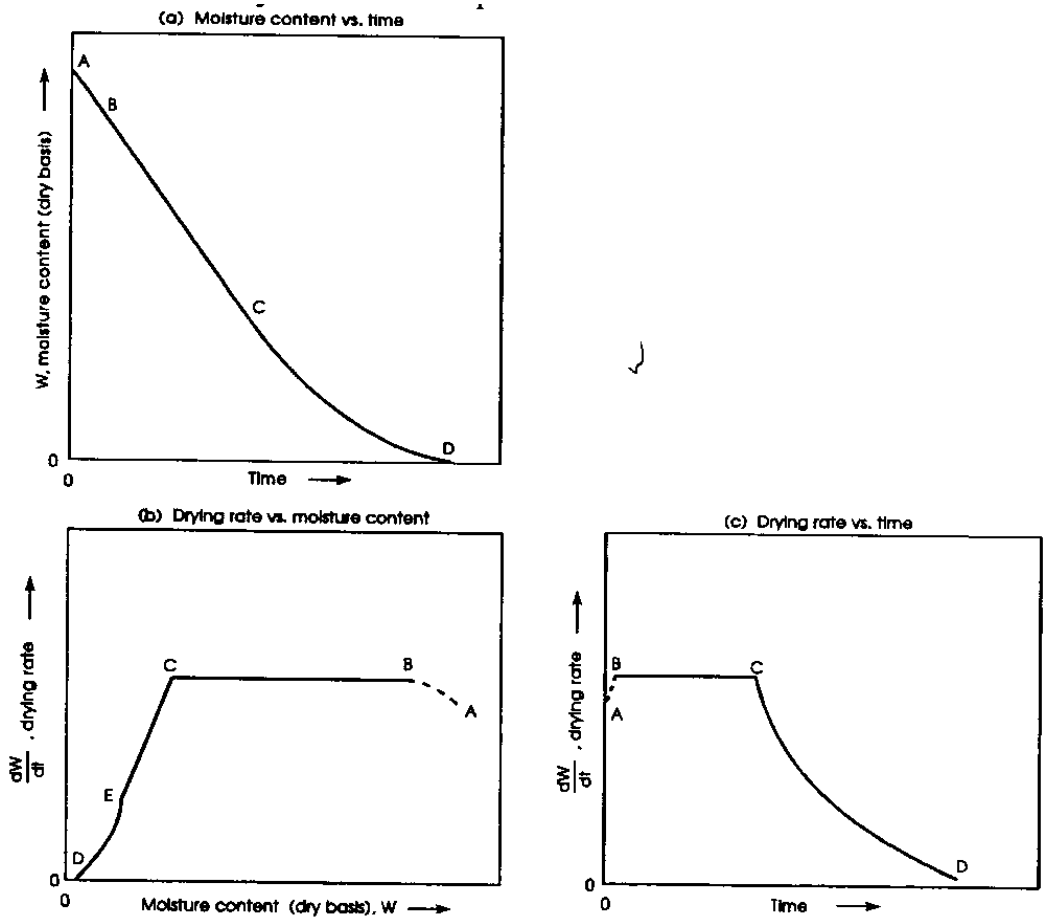

Figure 5.2 Periods of drying

5.4 *Constant-rate period.*

In the constant-rate period, moisture movement within the solid is rapid enough to maintain a saturated condition at the surface, and the rate of drying is controlled by the rate of heat transferred to the evaporating surface. Drying proceeds by diffusion of vapour from the saturated surface of the material across a stagnant air film into the environment. The rate of mass transfer balances the rate of heat transfer and the temperature of the saturated surface remains constant. The mechanism of moisture removal is equivalent to evaporation from a body of water and is essentially independent of the nature of the solids.

If heat is transferred solely by convection and in the absence of other heat effects, the surface temperature approaches the wet-bulb temperature. However, when heat is transferred by radiation, conduction, or a combination of these and convection, the temperature at the saturated surface is between the wet-bulb temperature and the boiling point of water. Under these conditions, the rate of heat transfer is increased and a higher drying rate results.

When heat is transferred to a wet solid by convection to hot surfaces and heat transfer by convection is negligible, the solids approach the boiling-point temperature rather than the wet-bulb temperature. This method of heat transfer is utilized in indirect dryers. Radiation is also effective in increasing the constant rate by augmenting the convection heat transfer and raising the surface temperature above the wet-bulb temperature.

Wet bulb temperature is the dynamic equilibrium temperature attained by a water surface when the rate of heat transfer to the surface by convection is equal to the rate of mass transfer away from the surface.

When the heat for evaporation in the constant-rate period is supplied by a hot gas, a dynamic equilibrium establishes the rate of heat transfer to the material and the rate of vapour removal from the surface

$$dW / dt = \alpha A \Delta T / \Delta H = kA\Delta P \quad \textbf{(5.2)}$$

where
- dW/dt = drying rate, kg water/s
- α = total heat-transfer coefficient, J/(m^2 s K)
- A = area for heat transfer and evaporation, m^2
- ΔH = latent heat of evaporation at T_s, J/kg
- k = mass-transfer coefficient, kg/(s m^2 atm)
- ΔT = $T - T_s$
- T = gas (dry-bulb) temperature, K
- Δp = $p_s - p$
- p_s = vapour pressure of water at surface temperature T_s, atm
- p = partial pressure of water vapour in the gas, atm

The magnitude of the constant rate depends upon three factors:

- the heat- or mass-transfer coefficient
- the area exposed to the drying medium
- the difference in temperature or humidity between the gas stream and the wet surface of the solid

All these factors are the *external* variables. The *internal* mechanism of liquid flow does not affect the constant rate.

For drying calculations, it is convenient to express equation (5.2) in terms of the decrease in moisture content rather than in the quantity of water evaporated. For evaporation from a tray of wet material, if no change in volume during drying is assumed, equation (5.2) becomes

$$dW / dt = (\alpha / \rho_s d\Delta H)(T - T_s) \quad \textbf{(5.3)}$$

where
- dW/dt = drying rate, kg water/(s-kg dry solids)
- α = total heat-transfer coefficient, J/(m^2 s K)
- ρ_s = bulk density dry material, kg/m^3
- d = thickness of bed, m
- ΔH = latent heat of vaporization, J/kg
- T = air temperature, K
- T_s = evaporating surface temperature, K.

For constant rate drying, $(T-T_s)$ is constant, hence the drying of a particle can be described by integrating this equation and using that for $t=0$, $W=W_i$, the initial moisture content:

$$\frac{W}{W_i} = 1 - \frac{t}{\tau}$$

(5.4)

where

$$\tau = \frac{\rho_s d \Delta H W_i}{\alpha (T_s - T)}$$

(5.5)

the time to completely dry a feed particle.
The average moisture content of the leaving solids is defined by:

$$\overline{W} = \int_{t=0}^{t=\tau} W E(t) dt$$

(5.6)

where E(t) is the residence time distribution of the solids:

$$E(t) = \frac{1}{\tau_r} e^{-t/\tau_r}$$

(5.7)

in which τ_r is the residence time of the particles in the bed.
Combination of equations (5.4) and (5.6) and integrating from t=0 to τ gives:

$$\frac{W}{W_i} = 1 - \frac{1 - e^{-\tau/\tau_r}}{\tau / \tau_r}$$

(5.8)

Example 5.1.

A fluidized bed dryer reduces the moisture content of a powdery ore from W_i = 0.17 to W = 0.02. The drying takes place at 80 °C, the feed rate of the dry solids is 15 kg/s.
In a small batch experiment at 80 °C the feed solids dried at a constant rate to completion in τ = 127 s.
The cross sectional area of the bed is 5 m^2, the bed porosity 0.45 and the solids density 2500 kg/m^3. What is the height of the fluidized bed?

Solution:

Using equation (5.8) gives:

$$\frac{0.02}{0.17} = 1 - \frac{1 - e^{-127/\tau_r}}{127 / \tau_r}$$

from which τ_r = 500 s.
The weight of the bed is 15 kg/s * 500 s = 7500 kg.
The height of the bed is then:

$$H = \frac{G}{A_c(1-\varepsilon)\rho_s} = \frac{7500}{5(1-0.45)2500} = 1.09m$$

An equation similar to (5.3.) can be written for the through-circulation case:

$$dW / dt = (\alpha A_b / \rho_s \Delta H)(T - T_s)$$

(5.9)

where A_b = m^2 of heat-transfer area/m^3 of bed.

The values of ρ_s, and/or A_b must be known in order to use equations (5.3) and (5.4). The value of A_b is difficult to estimate without experimental data. When the void fraction is known, A_b can sometimes be estimated from the following relationships:
For spherical particles,

$$A_b = \frac{6(1-\varepsilon)}{d_{vs}}$$

(5.10)

For uniform cylindrical particles,

$$A_b = \frac{4(0.5D + L)(1-\varepsilon)}{DL}$$

(5.11)

where ε = void fraction
d_{vs} = volume/surface diameter of spherical particles
D = diameter of cylinder
L = height of cylinder

For cylindrical particles that are long relative to their diameter, the term 0.5D in equation (5.6) can be neglected.

5.5 *Falling-rate period.*

The falling-rate period begins at the critical moisture content when the constant-rate period ends. When the falling moisture content is above the critical moisture content, the whole drying process will occur under constant-rate conditions. If, however, the initial moisture content is below the critical moisture content, the entire drying process will occur in the falling-rate period. This period is usually divided into two zones:

(i) the zone of *unsaturated surface* drying and
(ii) the zone where *internal moisture movement* is the controlling factor

In the first zone, the entire evaporating surface can no longer be maintained and saturated by moisture movement within the solid.
The drying rate decreases from the unsaturated portion, and hence the rate for the total surface decreases. Generally, the drying rate depends on factors affecting the diffusion of moisture away from the evaporating surface and those affecting the rate of internal moisture movement. As drying proceeds, the point is reached where the evaporating surface is unsaturated. The point of evaporation moves into the solid, and the dry process enters the second falling-rate period. The drying rate is now governed by the rate of internal moisture movement; the influence of external variables diminishes. This period usually predominates in determining the overall drying time to lower moisture content.

5.6 *Liquid diffusion.*

Diffusion-controlled mass transfer is assumed when the vapour or liquid flow conforms to Fick's second law of diffusion. This is stated in the unsteady-state-diffusion equation using mass-transfer notation as

$$\delta_c / \delta_t = D(\delta^2 c / \delta x) \qquad \textbf{(5.12)}$$

where c = the concentration of one component in a two-component phase of A and B
t = the diffusion time
x = distance in the direction of diffusion
D = diffusivity

For slab-sheet solids, this equation can be solved and for long drying times the simplified solution becomes:

$$-\frac{dW}{dt} = \frac{\pi D}{4d^2}(W - W_e) \qquad \textbf{(5.13)}$$

where dW/dt = drying rate, kg/s
d = thickness of the layer through which diffusion occurs
W_e = the equilibrium moisture content (the moisture content the material attains after extended exposure to air at a constant temperature and humidity).

Equations (5.12) and (5.13) hold only for a slab-sheet solid whose thickness is small relative to the other two dimensions. For other shapes, other equations can be derived.

5.7 *Capillary theory.*

If the porous size of a granular material is suitable, moisture may move from a region of high to one of low concentration as the result of capillary action rather than by diffusion. The capillary theory assumes that a bed of nonporous spheres is composed of particles surrounding a space called a pore. These pores are connected by passages of various sizes. As water is progressively removed from the bed, the curvature of the water surface in the interstices of the top layer of spheres increases and a suction pressure because of this curvature exists. As the removal of water continues, the suction pressure attains a value in which air is drawn into the pore spaces between successive layers of spheres. This entry suction or suction potential is a measure of the resultant forces tending to draw water from the interior of the bed to the surface.
As drying proceeds, the surface moisture evaporates, causing retreat of the surface menisci until the suction potential reaches a critical value. At that point, the pores of the surface will open, air will enter, and the moisture will redistribute itself with a slight lowering of the suction potential. As evaporation proceeds, the suction potential again increases until a slightly higher entry value is reached, when a further redistribution occurs.
The drying rate curve (Fig 5.2b) can be analyzed in terms of capillary theory. In region BC, there is a loss of moisture with a gradual increase in suction and emptying of the bulk of the larger pores in the solid. In region CE, there is an increase in suction as the moisture content decreases and finer pores are opened. Section ED represents a condition in which moisture is being removed by vapour diffusion from the interior of the body, although there is still sufficient water in the bed to give rise to capillary forces.

5.8 *Estimation of total drying time.*

Estimates of both the constant-rate and the falling rate drying periods are needed to estimate the total drying time for a given operation. If estimates for these periods are available, the total drying time can be obtained by summing these individual drying times. It is often difficult, however, to get a good estimate of critical moisture content, thus reducing the number of good estimates of total drying time.

5.9 *Analysis of data.*

When experiments are carried out to select a suitable dryer and to obtain design data, the effect of changes in various external variables is studied. These experiments should be conducted in an experimental unit that simulates the large-scale dryer from both the thermal and material-handling aspects, and only material which is truly representative of full-scale production should be used.
Data expressing moisture content in terms of elapsed time should be obtained and the results plotted as shown in Figure 5.3. For purpose of analysis, the moisture-time curve must be differentiated graphically or numerically and the drying rates so obtained plotted to determine the nature and extent of the drying periods in the cycle.

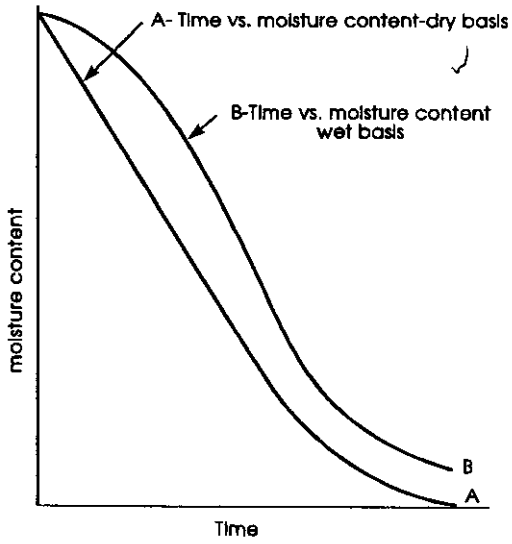

Figure 5.3 Drying time curves

It is customary to plot drying rate versus moisture content as shown in Figure 5.2b. Although instructive, this type of plot gives no information on duration of the drying periods. These are better shown by plots similar to Fig. 5.2c, in which drying rate is plotted as a function of time on either arithmetic or logarithmic co-ordinates. Logarithmic plots permit easy reading at low moisture contents or long times.

Tests on plant-scale dryers are usually carried out to obtain design data for a specific material, to select a suitable dryer type, or to check present performance of an existing dryer with the objective of determining its capacity potential. In these tests, overall performance data are obtained and the results used to make heat and material balances and to estimate overall drying rates or heat-transfer coefficients.

Generally the minimum data to be taken in order to calculate the performance of a dryer are:

- Inlet and outlet moisture contents
- Inlet and outlet gas temperatures
- Inlet and outlet material temperatures
- Feed rate
- Gas rate
- Inlet and outlet humidities
- Retention time or time of passage through the dryer
- Fuel consumption

Whenever possible moisture contents and temperatures should be measured at various points within the dryer.
Typical experimental and calculated results of a drying test for a continuous adiabatic convection dryer are shown in Figure 5.4.

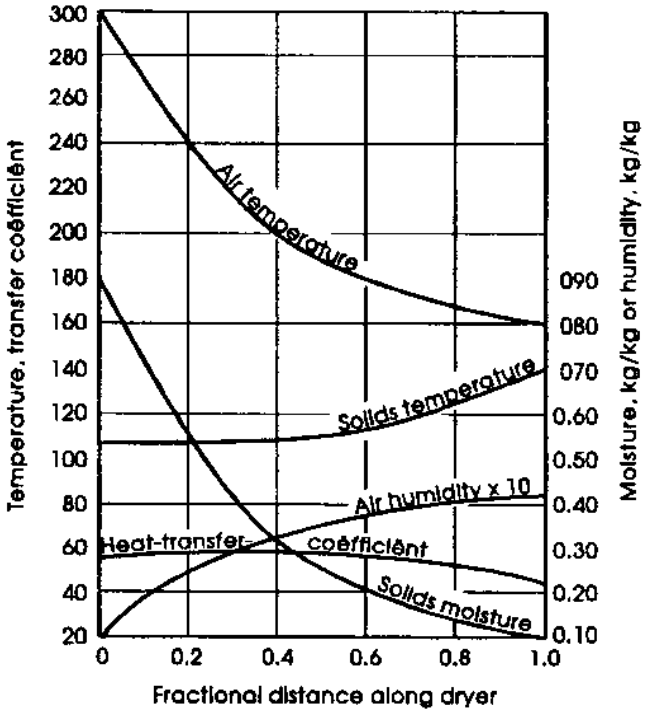

Figure 5.4 Typical results of dryer performance test.

Test data as elaborate as those shown are not usually justified economically except when basic studies, aimed at clarifying the effect of
operating variables, are being carried out in order to arrive at a reliable design procedure. The completeness of the information which is sought in any given test depends on the ultimate use of the data.
In any case data for at least two sets of operating conditions are needed if a good analysis of dryer performance is to be made.
Results of drying tests can be correlated empirically in terms of overall heat-transfer coefficient or length of a transfer unit as a function of operating variables. The former is generally applicable to all types of dryers, while the latter applies only in the case of continuous dryers.
The number of transfer units in any direct dryer is given by:

$$N_t = (T_1 - T_2) / \Delta T_m \qquad \textbf{(5.14)}$$

where N_t = number of transfer units
T_1 = inlet gas temperature
T_2 = exit gas temperature
ΔT_m = mean temperature difference between gas and solids through the dryer, K.

The heat-transfer coefficient along the dryer is lower at the discharge end (Fig. 5.4) because of the internal resistance to moisture movement in the later stages of drying. When drying

data are expressed in terms of overall performance, care and judgment should be exercised in extrapolating the results to other conditions, particularly conditions of different feed and product moisture.
If, for example, the overall heat-transfer coefficients from the data of Figure 5.4, were used to predict a dryer design for reducing the product moisture below 10 percent, the design would be in error.
Obviously, this problem can be circumvented by making sure that the final moisture in the experiments is below that desired in the product.
In any capacity test to determine the potential of a plant dryer, the effects of the following variables should be studied:

- Effect of increased temperature. This is often the simplest way to achieve increased capacity.
- Effect of increased final moisture. Because of the marked increase in drying time required to dry to low moisture contents, the permissible maximum final moisture should always be established.
- Effect of increasing air velocity should be determined. Frequently, higher air rates are necessary to provide the required additional heat at higher capacities.
- Uniformity of air flow should be established. Air-flow maldistribution can seriously reduce dryer capacity and efficiency.
- Possible benefits from air recirculation should be considered.

Example 5.2. [5.3]

A granular material containing 40% moisture (wet basis) is fed to a countercurrent rotary dryer at a temperature of 295 K and is withdrawn at 305 K containing 5% moisture. The air supplied, which contains 0.006 kg water vapour per kg of dry air, enters at 385 K and leaves at 310 K. The dryer handles 0.125 kg/s wet stock.
Assuming that the radiation losses amount to 20 kJ/kg dry air used, determine the weight of dry air supplied to the dryer per second and the humidity of the air leaving it.

Latent heat of water vapour at 295 K = 2449 kJ/kg
Specific heat of dried material = 0.88 kJ/kg K
Specific heat of dry air = 1.00 kJ/kg K
Specific heat of water vapour = 2.01 kJ/kg K
Specific heat of liquid water = 4.18 kJ/kg K

Solution:

This problem can be solved by making a heat balance over the system. 273 K will be chosen as the reference temperature and it will be assumed that the flow of dry air is m kg/s.

Heat in

(i) Air
m kg/s dry air enter containing 0.006 m kg/s water vapour per kg dry air and hence the energy in this stream is:

$$[(1.00m) + (0.006m * 2.01)](385-273) = 113.35\ m\ kW$$

(ii) Wet solid

0.125 kg/s wet solids enter containing 0.40 kg water/kg wet solid (assuming 40% moisture on a wet basis), hence:

mass flow of water = (0.125*0.40) = 0.050 kg/s

mass flow of dry solids = (0.125 - 0.050) = 0.075 kg/s

Hence the energy in this stream is:

[(0.050*4.18)+(0.075*0.88)](295-273) = 6.05 kW

Heat out

(i) Air

Energy in exit air is:

[(1.00m)+(0.006m*2.01)](310-273) = 37.45m kW

Mass flow of dry solids is:

0.075 kg/s containing 0.05 kg water/kg wet solids (assuming 5% moisture on a wet basis).

Using equation (5.1), the moisture content on a dry basis is:

$W_d = W_w/(1-W_w) = 0.05/0.95 = 0.0526$ kg water/kg dry solids.

Hence water in dried solids leaving is:

0.0526*0.075 = 0.0039 kg/s,

and the water evaporated into the gas stream is:

(0.050-0.039) = 0.0461 kg/s.

Assuming evaporation takes place at 295 K, energy water vapour is:

0.046[2.01(310-295)+2449+4.18(295-273)] = 118.53 kW,

and the total energy in this stream is:

(118.53+37.45m) kW.

(ii) Dried solids

The dried solids contain 0.0039 kg/s water and hence the energy content of this stream is:

[(0.075*0.88)+(0.0039*4.18)*(305-273)] = 2.63 kW.

(iii) Losses

These amount to 20 kJ/kg dry air or 20m kW.

Balance

113.35m + 6.05 = 118.53 + 37.45m + 2.63 + 20m

from which m = 2.06 kg/s.

The amount of water in the outlet stream is:

(0.006*2.06)+0.0461 = 0.0585 kg/s,

and the humidity is:

0.0585/2.07 = 0.0283 kg/kg dry air.

References:

[5.1] Perry, R.H., Green, D.
Perry's Chemical Engineer's Handbook
McGraw-Hill, 1984

[5.2] Hougen., McCauley., Marshall,
Trans. Am. Inst. Chem. Eng., 36, 193, 1940

[5.3] Coulson, J.M., Richardson, J.F., Backhurst, J.R., Harker, J.H.
Chemical Engineering, vol. 5
Pergamon Press, 1979

CHAPTER 6. Cyclones.

The separation of solid bodies is named grading or classification. It can be defined as splitting up a mixture into two or more fractions, each of which is more uniform in a certain property than the original mixture.
When use is made of differences in the velocity of particles in a fluid, we speak of pneumatic or hydraulic classification.
Pneumatic classification is sometimes called wind-sifting; it can be carried out in the following ways [6.1]:

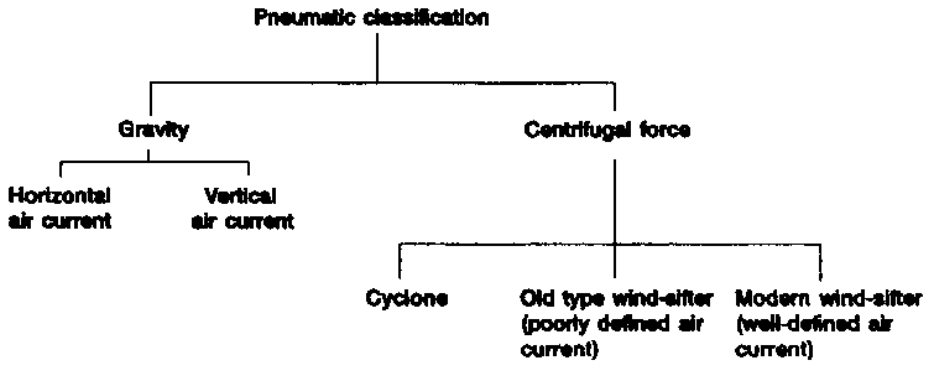

Figure 6.1 Pneumatic classification.

Classification in an air current is sometimes an attractive technique and it is generally not very expensive.
If the particles become small, however, separation from the air flow becomes increasingly difficult and a centrifugal force may be necessary to achieve the desired separation. This can be accomplished in a cyclone, of which the dimensions and operational conditions are so chosen that the fine fraction passes through the overflow and the coarse fraction is obtained in the underflow.
Hydraulic classification bears great resemblance to wind-sifting and it can also be carried out under the force of gravity or by means of a centrifugal force (see Figure 6.2).

The use of hydro cyclones has the advantage of simplicity and flexibility, so that the results may be modified by altering operating conditions. As opposed to many other types of equipment, hydro cyclones are better for classifying than for clarifying. The reason is that the high shearing stresses in a hydro cyclone promote the suspension of the particles and oppose flocculation. A disadvantage is that both the coarse and the fine fractions are obtained as suspensions of fairly high dilution. Moreover, the viscosity of the fluid should not be too high.

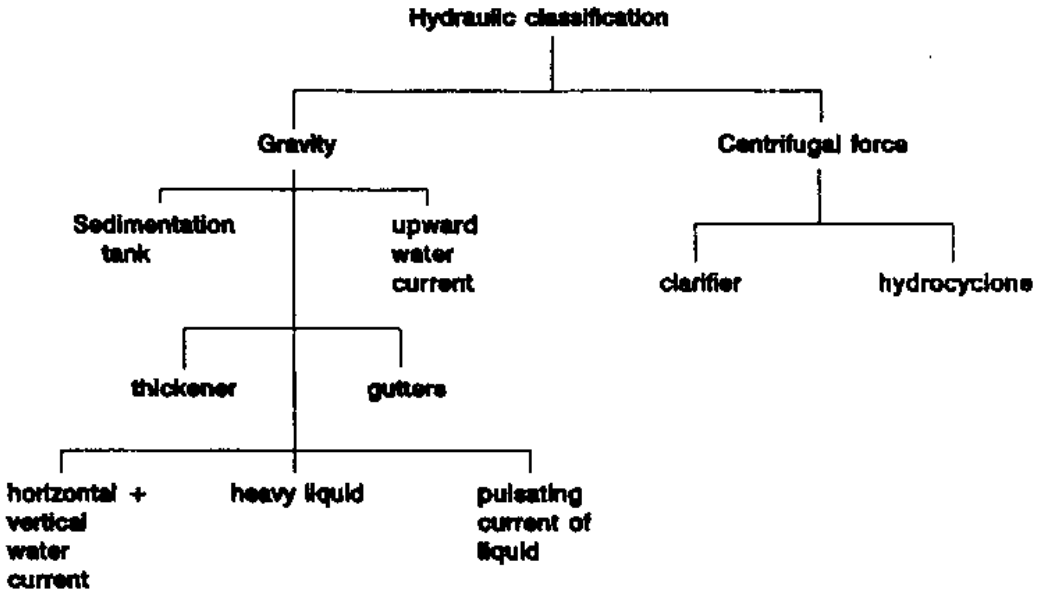

Figure 6.2 Hydraulic classification.

6.1 *Centrifugal separation.*

The rate of settling in a fluid can be greatly increased if centrifugal rather than gravitational forces are employed. In the cyclone separator (Figure 6.3), the fluid is introduced tangentially into a cylindrical vessel; clean fluid is taken off through a central outlet at the top. The solids are thrown outward against the cylindrical wall of the vessel and are collected in the conical base.

This separator is very effective, unless the fluid contains a large proportion of particles less than 10 micron in diameter.

The fluid in the cyclone moves spirally downward, gradually approaching the central portion of the separator and then rises and leaves through the central outlet at the top. The tangential component of the velocity of the fluid appears to predominate through the whole depth, except within a highly turbulent central core of diameter about 0.4 times that of the fluid outlet pipe. The radial component of the velocity acts inwards, and the axial component is away from the fluid inlet near the walls of the separator but is in the opposite direction in the central core. Pressure measurements indicate a relatively high pressure throughout, except of a region of reduced pressure corresponding to the central core. Any particle is therefore subjected to two opposing forces in the radial direction: the centrifugal force that tends to throw it to the walls and the drag of the fluid that tends to carry the particle away through the fluid outlet. Both of these forces are a function of the radius of rotation and of the size of the particles, with the result that particles of different sizes tend to rotate at different radii. As the outward force on the particle increases with the radial component, the separator should be designed so as to make the tangential velocity as high as possible and the radial velocity low, if particles of small sizes are to be collected in the underflow. This is generally realised by introducing the fluid at high tangential velocity and making the height of the separator large.

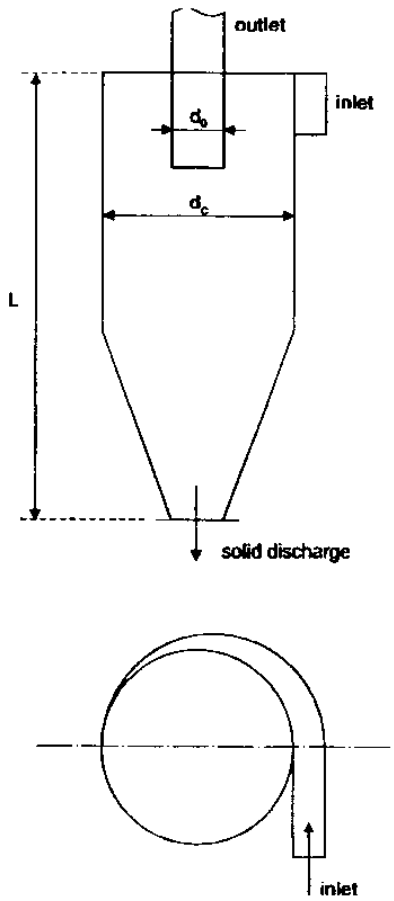

Figure 6.3 Schematic diagram of a cyclone separator.

A technical limitation is that the combination of solids and fluid velocities of more than 40 m/s create excessive wear. Therefore design tangential velocities are often maximized at 25 m/s.

The radius at which a particle will rotate within the cyclone corresponds to the position where the net radial force on the particle is zero. The two forces acting are the centrifugal force outwards and the frictional drag of the fluid acting inwards.

Let's consider a spherical particle of diameter d, rotating at radius r. Then the centrifugal force is:

$$\frac{\pi d^3}{6}(\rho_s - \rho)\frac{u_t^2}{r} \qquad \textbf{(6.1)}$$

Where ρ_s = particle density
ρ = density of the fluid
u_t = tangential component of the velocity of the fluid

It is assumed that there is no slippage between the fluid and the particle in the tangential direction.

If the radial velocity is low, the inward radial force due to friction will be equal to the Stokes drag, equation (1.1):

$$\frac{\pi d^3(\rho_s - \rho)}{6}\frac{u_t^2}{r} = 3\pi\mu d u_r$$

or

$$\frac{u_t^2}{r} = \frac{18\mu}{d^2(\rho_s - \rho)}u_r \qquad \textbf{(6.2)}$$

Now the free falling velocity of the particle is given by equation (1.12) as:

$$v_0 = \frac{1}{18}\frac{d^2(\rho_s - \rho)g}{\mu} \qquad \textbf{(6.3)}$$

Substituting in equation (6.2):

$$\frac{u_t^2}{r} = \frac{u_r}{v_0}g$$

or

$$v_0 = \frac{u_r}{u_t^2}rg \qquad \textbf{(6.4)}$$

So the separator cut can be defined in terms of the laminar terminal falling velocity: the higher the terminal falling velocity, the greater the radius at which it will rotate, and the easier it is to separate. If we assume that a particle will be separated, provided it tends to rotate outside the central core of diameter $0.4d_0$, the terminal falling velocity of the smallest particle which will be retained is found by substituting $r = 0.2d_0$ in equation (6.4), i.e.

$$v_0 = 0.2\frac{u_r}{u_t^2}d_0 g \qquad \textbf{(6.5)}$$

In order to calculate v_0, it is necessary to evaluate u_r and u_t for the region outside the central core. The radial velocity u_r is found to be approximately constant at a given radius and to be given by the volumetric rate of flow of the fluid to the outlet (which is almost the same as the flow through the inlet), divided by the cylindrical area for flow at the radius *r*. So, if *G* is the mass rate of flow of the fluid through the separator, the linear velocity in the radial direction at a distance *r* from the axis is given by:

$$u_r = \frac{G}{2\pi r L \rho} \tag{6.6}$$

where L is the length of the separator.
The tangential velocity is found to be inversely proportional to the square root of the radius at all depths (using Bernoulli's equation and conservation of momentum). Then, if u_t is the tangential component of the velocity at radius r, and u_{t0} is the corresponding value at the circumference of the separator:

$$u_t = u_{t0}\sqrt{\frac{d_c}{2r}} \tag{6.7}$$

Of course, u_{t0} is approximately equal to the velocity with which the fluid enters the cyclone. If these values for u_r and u_t are now substituted into equation (6.5), the terminal falling velocity of the smallest particle which the separator will retain is given by:

$$v_0 = 0.2\frac{G d_0 g}{\pi \rho L d_c u_{t0}^2} \tag{6.8}$$

If the cross-sectional ea of the inlet is A_i, then $G = A_i \rho u_{t0}$ and:

$$v_0 = 0.2\frac{A_i^2 \rho d_0 g}{\pi L d_c G} \tag{6.9}$$

A small inlet and outlet therefore result in the separation of smaller particles, but as the pressure drop over the separator varies with the square of the inlet velocity and the square of the outlet velocity, the practical limit is set by the permissible pressure drop/fluid velocity. The depth and diameter of the body should be as large as possible, because the former determines the radial component of the fluid velocity and the latter controls the tangential component at any radius. In general, the larger the particles, the larger should be the diameter of the separator because the greater is the radius at which they rotate.
Because the separating power of the cyclone is directly related to the throughput of fluid, the separator is not very flexible, though its efficiency can be improved at low throughputs by restricting the area of the inlet, and hence increasing the inlet velocity. Generally, however, it is better to use a number of cyclones in parallel and to keep the load on each approximately the same.
Because the vertical component of the velocity in the cyclone is downwards everywhere outside the core, the particles will rotate at a constant distance from the centre and move continuously downwards until they settle in the conical base. Continuous removal of solids is desirable so that the particles do not get entrained again in the fluid stream due to relatively

low pressures in the central core. Entrainment is reduced to a minimum if the cyclone has a deep conical base of small angle.

Example 6.1.

A cyclone separator, 0.3 m in diameter and 1.2 m long, has a circular inlet 75 mm in diameter and an outlet of the same size. If the gas enters at 1.5 m/s, at what particle size will the theoretical cut occur?

Viscosity of air	$0.018\ 10^{-3}$ Ns/m^2
Density of air	1.3 kg/m^3
Density of particles	2700 kg/m^3

Solution.

The cross-sectional area $A_i = 4.4\ 10^{-3}$ m^2. The mass flow rate of the gas becomes then $G = 1.5$ m/s * $4.4\ 10^{-3}$ m^2 * 1.3 kg/m^3 = $8.6\ 10^{-3}$ kg/s.

Using equation (6.9), the free-falling velocity v_0 can be calculated:

$$v_0 = 0.2\frac{A_i^2 \rho d_0 g}{\pi L d_c G} = 3.8\ 10^{-4}\ \text{m/s}$$

Stokes law (1.3) is now used to find the particle diameter

$$d_{cut} = \sqrt{\frac{u_0 * 18\mu}{g\rho_s}}$$
$$= 2.17\ 10^{-6}\ \text{m}$$

6.2 Optimum cyclone dimensions

There is no unique design manual for cyclones. The design is generally based on experiments by numerous authors. However, summarizing these experimental results leads to the following set of guidelines for the dimensions in liquid-solid cyclone systems:

$$\frac{l}{d_c} = 0.4$$
$$\frac{L}{d_c} = 5$$
$$\frac{d_i}{d_c} = 0.28$$
$$\frac{d_0}{d_c} = 0.34$$

(6.10)

where d_c = cyclone diameter
l = length of vortex finder
L = length of the cyclone
d_i = inlet diameter
d_0 = overflow outlet diameter

The vortex finder is the part of the overflow pipe projecting into the cyclone.
The manner in which the total length of the cyclone is divided over the cylindrical and conical sections is not highly critical. It appears that some preference must be given to a cone that is as long as possible, and that the top angle of the conical section should not exceed 30 degrees.
It should be noted that these data are only valid if an air core can develop in the centre of the cyclone.

6.3 Pressure drop in a cyclone

The resistance of a cyclone to the fluid flow is expressed by the flow resistance coefficient α, which is expressed as:

$$\alpha = \frac{Q}{A_f \sqrt{\frac{2\Delta p}{\rho}}} \qquad \textbf{(6.11)}$$

where Q = cyclone capacity (m^3/s)
A_f = area of the feed opening (m^2)
ρ = density of the fluid (kg/m^3)
Δp = pressure drop across the cyclone (N/m^2)

An important factor for the cyclone resistance is the Reynolds number:

$$\mathrm{Re} = \frac{\rho v_f d_c}{\mu} \qquad \textbf{(6.12)}$$

where v_f = feed entrance velocity (m/s)
d_c = cyclone diameter (m)
μ = fluid viscosity (Ns/m^2)

The resistance coefficient α for a certain cyclone is only dependent on the Reynolds number and the wall roughness. At higher Reynolds number, the flow resistance decreases as shown in Figure 6.4.

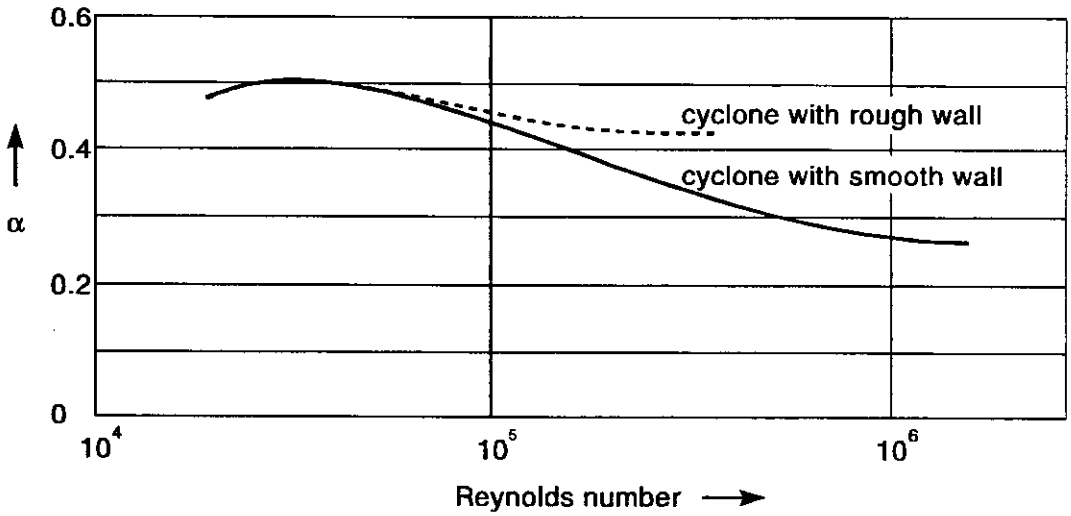

Figure 6.4 Resistance coefficient as a function of the Reynolds number.

6.4 Cyclone efficiency and classification curve.

The efficiency of the cyclone separator is greater for large than for small particles and increases with the throughput until the point is reached where excessive turbulence is created. If the cyclone is designed to separate a definite particle size, cyclone efficiency may be defined as the mass fraction of particles of that size that is recovered through the underflow. The classification curve (Figure 6.5) indicates the percentage of particles of a given particle size reporting in the apex discharge (underflow), leaving out of account in the calculation the solids in the feed which are initially contained in the volume of liquid released through the apex discharge.

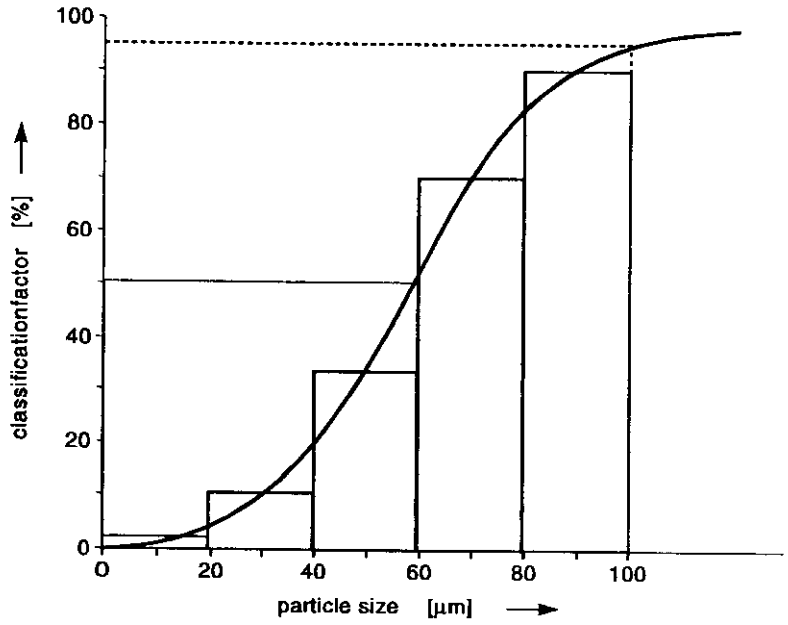

Figure 6.5 Cyclone classification curve.

A good classification curve is steep, which means that a relatively small amount of coarse material will end up in the overflow fraction and only a small amount of small particles will be discharged through the apex. A term that is often used is “separation size”. It relates to the size of particles of which 95% is caught. The 95% value is chosen arbitrarily, since the point of 100% is difficult to determine.
Unfortunately, different authors use different methods for representing cyclone performance. Wills [6.2] for example, represents cyclone efficiency by the performance or separation curve, which is in essence the same as the classification curve. He defines the “cutpoint” or “separation size” as that point for which 50 percent of particles in the feed of that size report to the underflow. This point is referred to as the d_{50} point.
The slope of the classification curve can be expressed by taking the points at which 75 and 25 percent of the feed particles report to the underflow. The efficiency of separation is reflected in the so-called imperfection:

$$\mathrm{I} = \frac{d_{75} - d_{25}}{2d_{50}} \tag{6.13}$$

Many mathematical models of hydro cyclones include the term “corrected d_{50}” taken from the “corrected” classification curve. It is assumed that in all classifiers, solids of all sizes are entrained in the liquid associated with the coarse product by short-circuiting in direct proportion to the fraction of the feed water reporting to the underflow.
For example, if the feed contains 16 t/h of material of a certain size, and 12 t/h report to the underflow, then the percentage of this size reporting to the underflow and plotted on the normal partition curve is 75%. However, if 25% of the feed water reports to the underflow, then 25% of the feed material will short-circuit with it, therefore 4 t/h of the size fraction will short-circuit to the underflow; and only 8 t/h reports to the underflow due to classification. The corrected recovery of the size fraction is thus:

$$\frac{12\text{-}4}{16\text{-}4} * 100 = 67\%$$

The uncorrected partition curve can therefore be corrected using the equation:

$$\mathrm{y}' = \frac{y - R}{1 - R} \tag{6.14}$$

where y’ is the corrected mass fraction of a particular size reporting to the underflow, y is the actual mass fraction of a particular size reporting to the underflow, and R is the fraction of the feed liquid that is recovered in the coarse product stream. Figure 6.6 shows uncorrected and corrected classification curves.

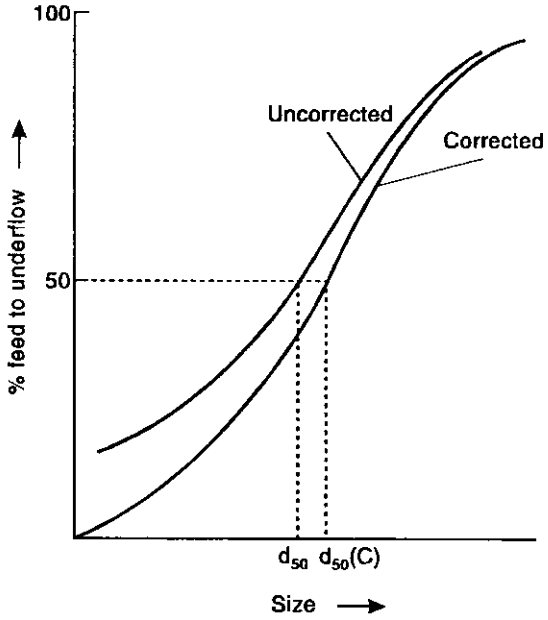

Figure 6.6 Uncorrected and corrected classification curves.

6.5 Influence of different variables on hydro cyclone operation.

Designing cyclones is generally based on experimental data. It is therefore useful to show some formulas that follow from the investigations of researchers. Bradley [6.3] lists various equations to calculate the cutpoint d_{50}. The oldest one is due to Dahlstrom:

$$d_{50} = 13.7 \frac{(d_0 d_i)^{0.68}}{Q^{0.53}(\rho_s - \rho)^{0.5}} \qquad \textbf{(6.15)}$$

where

	d_{50}	= cut point (micron)
	d_0	= overflow diameter (cm)
	d_i	= inlet diameter (cm)
	Q	= flow rate (m^3/h)
	ρ_s	= specific gravity of solids (gravity divided by gravity of water)
	ρ	= specific gravity of fluid (gravity divided by gravity of water)

Plitt [6.4] developed a mathematical equation for large diameter cyclones operating at high solids content (more than 3% vol.). The equation for the cut size is:

$$d_{50} = 14.8 \frac{d_c^{0.46} d_i^{0.6} d_0^{1.21} e^{0.063V}}{d_u^{0.71} h^{0.38} Q^{0.45} (\rho_s - \rho)^{0.5}} \qquad \textbf{(6.16)}$$

where d_{50} = "corrected" cut point (micron)
d_c = cyclone diameter (cm)
d_i = inlet diameter (cm)
d_0 = overflow (vortex finder) diameter (cm)
d_u = apex diameter (cm)
Q = flow rate of feed slurry (m^3/h)
V = volumetric percentage of solids in the feed
h = distance of the bottom of vortex finder to the top of the underflow orifice (cm)
ρ_s = specific gravity of solids (gravity divided by gravity of water)
ρ = specific gravity of fluid (gravity divided by gravity of water)

Example 6.2.

The collection efficiency of a cyclone is 45% over the size range 0-5 micron, 80% over the size range 5-10 micron, and 96% for particles exceeding 10 micron. Calculate the efficiency of collection for the following dust:

weight distribution	50%	0-5 micron	
	30%	5-10 micron	
	20%	above 10 micron	

Solution.

For the collector:

size (micron)	0-5	5-10	>10
efficiency (%)	45	80	96

For the dust:

weight (%)	50	30	20	
Basis 100 kg dust, weight recovered: kg	22.5	24.0	19.2	total = 65.7

Overall efficiency = 65.7 %

References:

[6.1] Rietema,K. and Verver, C.G.
Cyclones in Industry
Elsevier publishing Company 1961

[6.2] Wills, B.A.
Mineral processing technology
Pergamon Press, 4th edition, 1988

[6.3] Bradley, D.

The hydrocyclone
Pergamon Press, Oxford, 1965

[6.4] Plitt, L.R.
A mathematical model of the hydrocyclone classifier
CIM Bull., 69, 114, dec. 1976

Chapter 7. Magnetic separation

Fig. MS.1 - Magnetic separation of ferrous metal from mixed MSW

1.1. Introduction

Magnets are the oldest aid to metal separation after hand sorting. The removal of magnetic material with permanent magnets has been known for hundreds of years. The first permanent magnets were found in nature and were used in navigation compasses for many centuries. Their specific use as an aid in identifying and separating ferrous and non-ferrous metals was discovered later. It was not until the discovery of the electric current or galvanism that electromagnetic fields could be generated. The work of Faraday (1791-1867) and Maxwell (1831-1879) made it possible to calculate magnetic fields and design magnetic separators.

1.2. Working principle

The working principle of a magnetic separator is based on the magnetic properties of materials and on the properties of the magnetic field. If a magnet with a shape as shown in Fig. MS.2 is placed in the proximity of mild steel, it will generate a magnetic field as indicated by the lines. The particle P, which has magnetic properties, will travel towards the magnetic pole. The force on the particle P depends on the difference between the field lines on one side of the particle compared to the other side of the particle, also called the gradient of the field. If the field lines were parallel (zero gradient), the particle P would turn like a compass needle, but would not move towards one of the magnetic

poles. The higher the gradient of the magnetic field, the greater the force on a magnetic particle. Therefore, high gradient magnetic fields are necessary to move weak or very weak magnetic particles.

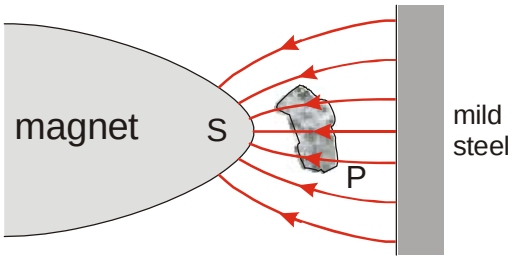

Fig. MS.2 - A particle in a magnetic field between a magnet and mild steel

In recycling, materials are usually subdivided into *magnetic* and *non-magnetic* materials. However, technically we distinguish *ferromagnetic* (strongly magnetic), *paramagnetic* (weakly magnetic), and non-magnetic materials. The separation of ferromagnetic materials from the others is always possible at high efficiency for all particle sizes, as long as the liberation is good and in case of dry separation of fines (< 5 mm) that the feed is not damp (= of a possibly fluctuating moisture content between entirely dry and fully soaked with water).

The magnetic separation of fines (< 3 mm) of paramagnetic and non-magnetic materials is in principle possible, but rarely applied in recycling practice (this contrary to minerals sorting where it is common in e.g. iron ore concentration and beach sand heavy minerals concentration). For larger sizes that are typical in recycling (>10 mm), the difference between para- and non-magnetic properties are only of use by applying electronic measurement and successive automatic sorting, since the weak magnetic forces are negligible compared to gravity for larger sized particles (> 5 mm). This and more is understood by a closer look into the physics of magnetism.

1.3. Theory of magnetism

When an electric current I [unit=A(mpere)] flows across a wire, a magnetic field H [A/m] (Ampere/meter) is generated around it (Fig MS.3 left). Its strength depends on the strength of the current and the distance *r* to the wire. A homogeneous field exists inside a coil of infinite length (Fig MS.3 middle).

MS.1.3.1. Magnetic moment

For the application of magnetic separation, we are interested mainly in *circulating* currents: loops of current. Magnetic theory shows that a loop of current produces a field as shown in Fig MS.3 (right: **S** [m^2] is a vector with a size equal to the area of the loop and pointing perpendicular to the loop in the direction of the *right-hand rule*):

$$\vec{H}(\vec{r}) = \frac{1}{4\pi}\left(3\frac{I\vec{S}\cdot\vec{r}}{r^5}\vec{r} - \frac{I\vec{S}}{r^3}\right) \quad [\text{A/m}]$$

[MS.1.1]

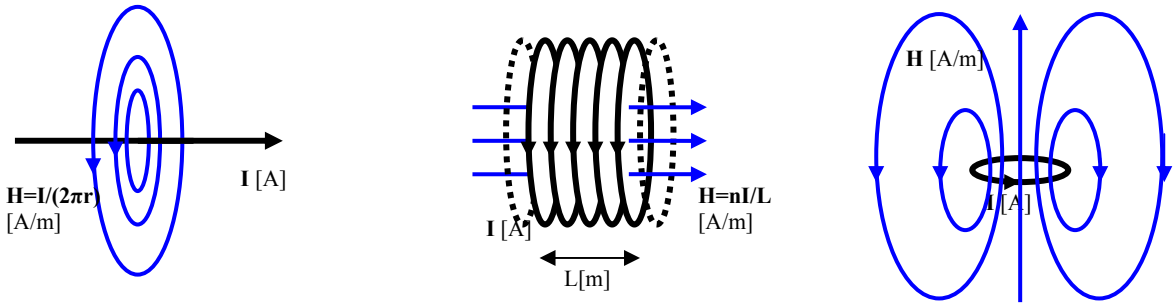

Fig. MS.3 – Relation between electric current and magnetic field

Magnetic fields created by an electric current act with a force on other electric currents (Fig MS.4 left). Consider a loop of current of strength I [A] around a small area with surface **S** [m^2] (Fig MS.4 middle).
The force of a magnetic field **H**(x,y,z) on such a loop of current is equal to

$$\vec{F} = \mu_0 I\vec{S}\nabla\frac{d\vec{H}}{d\vec{r}} = \mu_0 \frac{d(I\vec{S}\cdot\vec{H})}{d\vec{r}} \qquad [MS.1.2]$$

in which:

F = Force [N]
IS = magnetic (dipole) moment [Am^2]
IS·H = inner product of magnetic (dipole) moment and field
*d*H/*d*r = gradient of the component of the magnetic field that is parallel to **S** (perpendicular to the plane of the electric current) [A/m^2]

The coefficient μ_0 is the magnetic permeability in vacuum for a magnetic field. It has a constant value of $1.2566 \cdot 10^{-6}$ N/A^2. A magnetic field also produces a torque on a loop of current (Fig MS.4 right):

$$\vec{T} = \mu_0 I\vec{S} \times \vec{H} \qquad [MS.1.3]$$

in which:

T = Torque [Nm]
IS x H = vector product of magnetic (dipole) moment and field

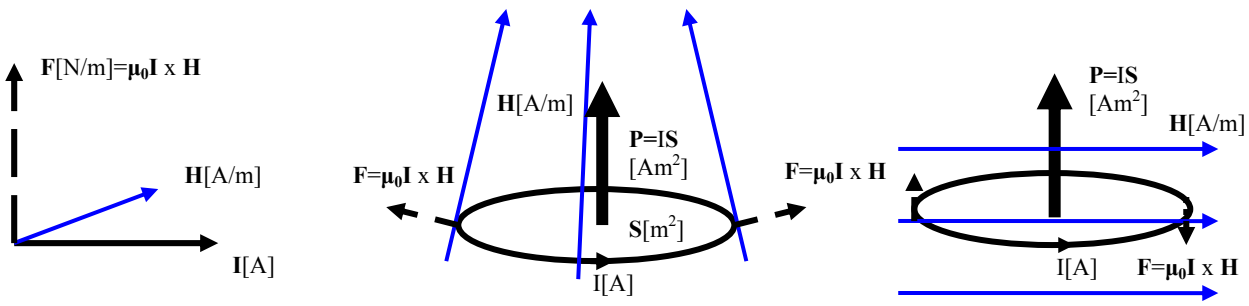

Fig. MS.4 – Force of a magnetic field on an electric current; concept of magnetic moment P=IS; force and torque on a loop of current.

The equations [MS.1.1-3] show that only the product of the current I and the surface of the loop S is relevant. For this reason, a new concept is defined: the magnetic moment $\mathbf{P}_m = I\mathbf{S}$, which is directed normal to the plane of the current, in the direction given by the *right hand rule*. The force and torque on a magnetic moment are:

$$\vec{F} = \mu_0 \frac{d(\vec{P}_m \cdot \vec{H})}{d\vec{r}} \qquad \text{[MS.1.4]}$$

$$\vec{T} = \mu_0 \vec{P}_m \times \vec{H} \qquad \text{[MS.1.5]}$$

MS.1.3.2. Magnetic materials

It turns out that the electrons inside atoms or ions behave like tiny loops of current. Therefore, every atom has a small magnetic moment $\mathbf{p}_m$. A material is magnetic if the magnetic moments (tend to) point in the same direction, as in the cross-section shown in Fig MS.5:

$$\vec{P}_m = \sum_{\text{atoms}} \vec{p}_m \qquad \text{[MS.1.6]}$$

The result of all the small loops of atomic currents is the same as if a loop of current runs along the surface of the material. In fact from the outside, we cannot distinguish a magnetic cylinder with an axial magnetic moment from a solenoid (an electric wire wound into a cylindrical coil): see Fig MS.6.

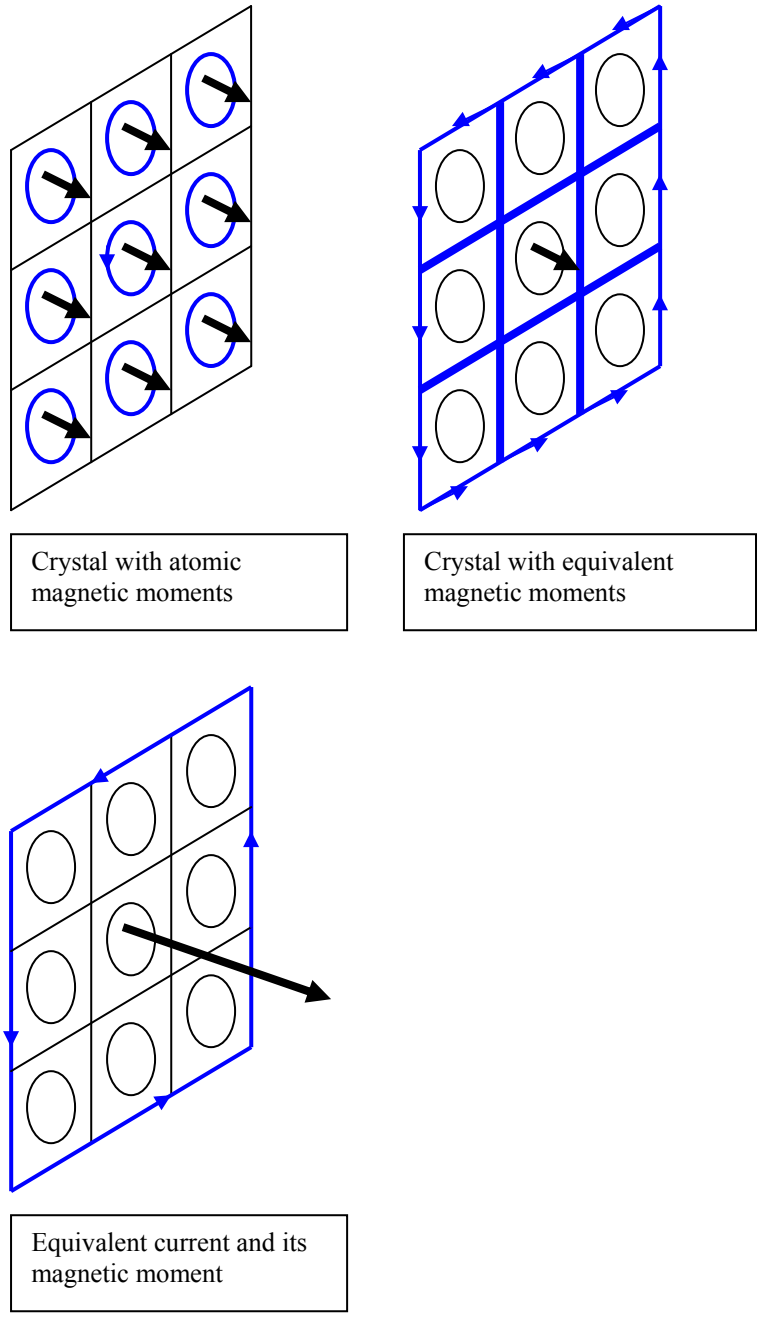

Fig. MS.5 – Left: cross-section of a crystalline material with atomic magnetic moments; Middle: enlarging S and reducing I while keeping P=IS fixed; Right: internal currents cancel and a surface current remains.

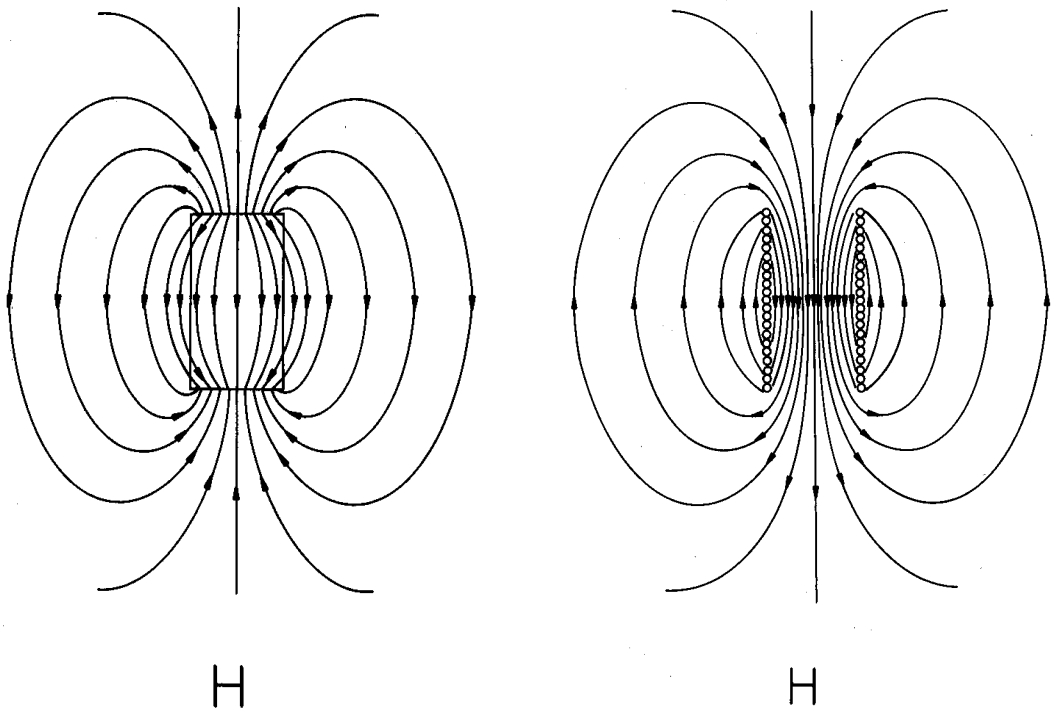

Fig. MS.6 – Magnetic field H of a cylindrical piece of axially magnetized material (left) and of a solenoid (right) are the same outside the cylinder volume..

Since the number of atoms, and so the number of atomic magnetic moments, is the same for each unit volume of a given type of material, the magnetic moment per unit volume is a material property, and it is indicated as *M*.

$$\vec{M} = \vec{P}_m/\mathrm{V} = \frac{1}{\mathrm{V}} \sum_{\text{atoms}} \vec{\mathrm{p}}_\mathrm{m} \qquad \text{[MS.1.7]}$$

Permanent magnets are materials in which all of the atomic magnetic moments are permanently locked in the same direction: such materials have an (almost) constant magnetization. They are used for making magnetic separators. Important examples of permanently magnetic materials are Barium-ferrites ($M \approx 0.25$-0.3 million A/m) and Iron-neodymium-boron ($M \approx 0.7$-1.0 million A/m). Comparing an axially magnetized permanent magnetic cylinder of a magnetization *M* with a solenoid with *n* turns per unit length of a wire carrying I Amperes, and assuming that both have the same cross-section S [m^2], we find that the magnetic moment is the same if

$$P_m = MV(\text{magnet}) = \mathrm{n}LIS(\text{solenoid}) = nIV(\text{solenoid}) \qquad \text{[MS.1.8]}$$

so if $M = \mathrm{n}I$ [A/m].

Unlike permanent magnets, most magnetic materials have atomic magnetic moments that orient themselves to the magnetic field, and so, the magnetization is a function of the internal magnetic field H inside the material.

Summarizing, we have the following results:

- Loops of current and small pieces of magnetic (magnetized) materials are magnetically equivalent: they are characterized by their magnetic moment $\mathbf{P}_\mathrm{m} = \mathrm{I}\mathbf{S} = \boldsymbol{M}\mathrm{V}$, which is a vector.

- Loops of current and small pieces of magnetic (magnetized) materials produce a magnetic field **H** that is proportional to their magnetic moment and looks like Fig MS.3 (right) and equation [MS.1.1].
- Any magnetic field acts on loops of current and small pieces of magnetic (magnetized) materials with a force and a torque given by equations [MS.1.2-4] and explained in Fig. MS.4.

In order to understand magnetic separation, one more concept needs to be introduced: how a magnetic field determines the magnetization of a material: how the atomic magnetic moments in a piece of material respond to a magnetic field. Permanent magnetic materials are easy: in this case there is almost no interaction and the magnetization M is frozen into the material. If a piece of permanent magnet is turned, all the atomic magnetic moments $\mathbf{p}_m$ turn with it, and so does the magnetization vector M and the magnetic moment $\mathbf{P}_m = M\mathrm{V}$ of the entire piece, regardless of the magnetic field (except for very strong fields).

Let us now turn to paramagnetic and (soft) ferromagnetic materials. These materials have no magnetization in a zero magnetic field. For small values of the magnetic field, the magnetization of these materials is linear with the *internal* magnetic field H, i.e., the field inside the piece of material. The (volumetric) magnetic susceptibility (χ = chi) is introduced according to:

$$\chi = \frac{M}{\mathrm{H}} \qquad \text{[MS.1.9]}$$

The value of χ is about 0.001 to 0.01 for paramagnetic minerals that can be recovered magnetically. For ferromagnetic materials χ can be as much as 1000 to a million (mild steel, mu-metal, for small values of H). Since χ is very large for ferromagnetic materials, the magnetization gets very large for small values of H and already at small H, all the atomic magnetic moments are fully parallel to the field: the material is then said to be magnetically saturated. After this point, the magnetization does not increase of course (see Fig. MS.7). Handbooks tabulate $\chi_s = \chi/\rho$ [m^3/kg] the so-called specific susceptibility (volumetric susceptibility divided by density of the material) rather than χ itself. In the same way, some sources give values for $M_s = M/\rho$ [Am^2/kg] instead of the magnetization. This is because in separation the magnetic force is often balanced against gravity. In rare cases, the magnetization M is given in [T(esla)], the unit for magnetic induction: in this case, the value in [A/m] is found by dividing by μ_0.

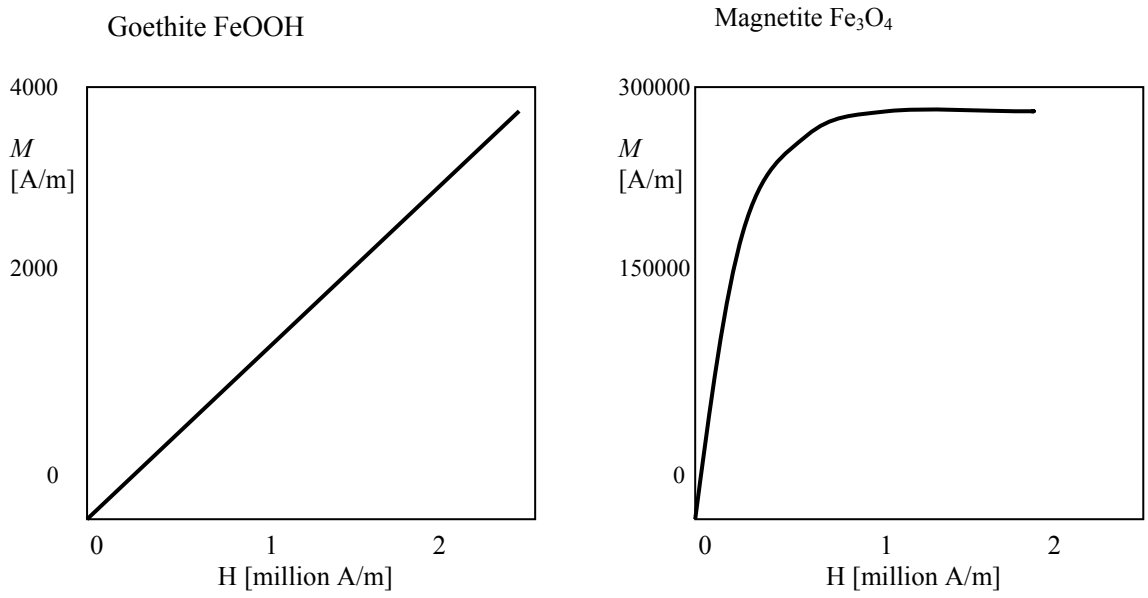

Fig. MS.7 – Magnetization of paramagnetic minerals (left) versus ferromagnetic materials (right) as a function of the internal magnetic field H.

MS.1.3.3. Forces on magnetic particles

In order to calculate the force on a magnetic particle in a magnetic field, we have to do the following steps:

- Compute the field H inside the magnetic particle
- Read the magnetization from the *M*-H curve and compute the magnetic moment $\mathbf{P}_m$ of the particle
- Use the equations for the force and torque

The computation of the magnetic field H inside a piece of magnetic material of some shape for a given external magnetic field (the field imposed by the separator magnet) is very technical, except for the case of weakly paramagnetic solids for which the internal magnetic field is almost the same as the field outside the particle. We therefore refer the interested reader to handbooks of magnetic theory. Here, we present as a fact that the force F for a particle having a certain χ, volume V and demagnetising (shape) factor N in an *external* field H is given by:

$$\begin{aligned}\vec{\mathrm{F}} &= \mu_0 \vec{P}_m \frac{d\vec{\mathrm{H}}}{d\vec{\mathrm{r}}} \\ &= \mu_0 \frac{V\vec{H}}{\frac{1}{\chi} + N} \frac{d\vec{\mathrm{H}}}{d\vec{\mathrm{r}}} \\ &= \mu_0 \frac{VH}{\frac{1}{\chi} + N} \frac{d\mathrm{H}}{d\vec{\mathrm{r}}}\end{aligned} \qquad \text{[MS.1.10]}$$

This is true as long as the magnetization of the material is not saturated. From here, we have two completely different cases:

1. Paramagnetic particles: $1/\chi >> N \approx 1/3$ (granular shape)
2. Ferromagnetic particles, in particular steel particles in recycling

For weakly paramagnetic materials having $\chi << 1$ Eq. [MS.1.10] becomes:

$$F = \mu_0 \chi H V \frac{dH}{dz} \quad \text{(Paramagnetic particles)} \qquad \text{[MS.1.11]}$$

where the magnetization of the particle is $M = \chi H$.

For ferromagnetic particles, the situation is more complicated. The most important application is the recovery of steel in recycling. Steel particles are mostly of a non-granular shape, e.g. resulting from steel plate or rods. This means that N is typically in the range 0.05-0.2 if the particles are oriented optimally with respect to the field (i.e, with the field parallel to one of the long axes of the particle). The saturation magnetization of ordinary steel is about 1.6 million A/m and the external fields delivered by separators is typically less than 300,000 A/m. For this reason, steel particles will be close to magnetic saturation near the separator magnet, as in pulley and drum separators. In these cases $M \approx 1.6$ million A/m while

$$F = \mu_0 M_{sat} V \frac{dH}{dz} \quad \text{(Saturated ferromagnetic particles)} \qquad \text{[MS.1.12]}$$

On the other hand, if the particles are far away from the separator magnet, as in cross belt and line belt separators, H will be much lower than 200,000 A/m and $1/\chi << N$. In this case, equation [MS.1.10] reduces to

$$F = \frac{1}{N} \mu_0 H V \frac{dH}{dz} \quad \text{(Non-saturated ferromagnetic particles)} \qquad \text{[MS.1.13]}$$

MS.1.3.4. Separator magnets

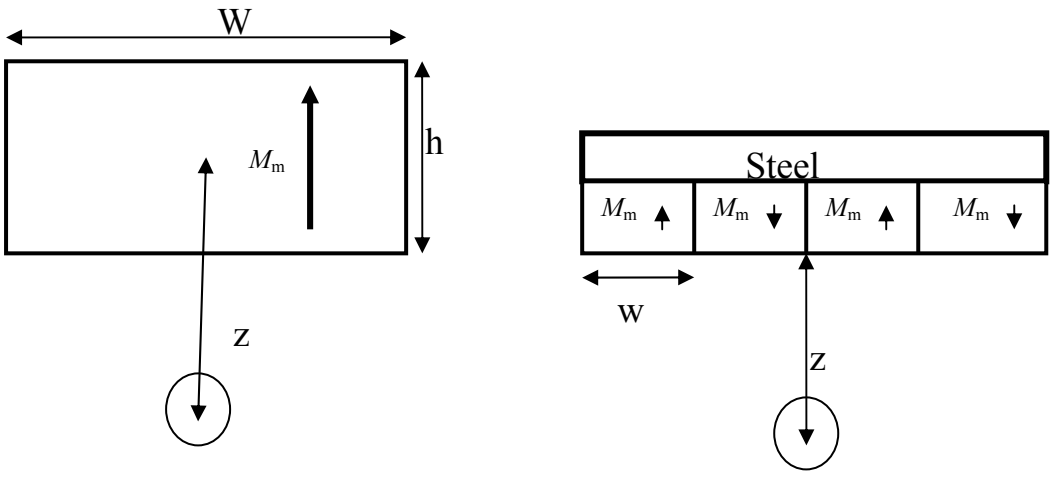

Fig. MS.8 – Dipole magnet (left) and multi-pole magnet (right).

Separator magnets in recycling consist of two fundamentally different designs: the multi-pole magnet and the dipole magnet. The multi-pole magnet has a high gradient and a short reach whereas the dipole magnet has a low gradient and a deep reach (typically >0.5 m). If a long dipole bar magnet with width W, height h and cross section S=Wh is centred at some position, with the south pole facing down (see Fig MS.8 left), the field at some point z [m] below the centre is approximately

$$\mathrm{H} = \frac{M_m S}{2\pi(\mathrm{W}^2/4 + z^2)} \quad [\mathrm{A/m}]; \qquad \frac{d\mathrm{H}}{dz} = \frac{z M_m S}{\pi\left(\mathrm{W}^2/4 + z^2\right)^2} \quad [\mathrm{A/m^2}]$$

[MS.1.14]

The field below a multi-pole magnet with pole width *w* (see Fig MS.8 right) decays exponentially with the distance z below the lower surface of the magnet:

$$\mathrm{H} = \frac{2M_m}{\pi} \mathrm{e}^{-\pi \mathrm{z/w}} \quad [\mathrm{A/m}]; \qquad \frac{d\mathrm{H}}{dz} = \frac{2M_m}{w} \mathrm{e}^{-\pi \mathrm{z/w}} \quad [\mathrm{A/m^2}]$$

[MS.1.15]

Both formulas [MS.1.14-5] are based on the use of permanent magnet poles with magnetization M_m. The best available permanent magnets have a magnetization of about M_m = 1 million A/m.

1.4. Concentration of ferrous metals

In recycling four main types of magnetic separators are frequently used for the separation of ferrous metals: cross belt, line belt, pulley and drum separators. For all types permanent magnets as well as electromagnets can generate the magnetic field. The advantage of permanent magnets is that they do not require energy to produce the magnetic field, as is the case with electromagnets. For this reason electromagnets are more and more replaced by permanent magnets. Only when an extremely high field strength is needed, e.g. for the concentration of weakly magnetic material or for heavy scrap, electromagnets are applied.

MS.1.4.1. Cross belt separator

Fig. MS.9 – Cross belt magnetic separator.

A cross belt separator uses permanent magnets and is mounted some distance above the conveyor. Ferrous metal is attracted and jumps up to the cross belt conveyer to be transported outside the magnetic field where it drops of. It is suitable for the removal of smaller amounts of ferrous metals (de-contamination) or for smaller installations. When the amount of ferrous metal is substantial, line belt, pulley or drum separators are often preferred. Cross belt and line belt separators are able to produce relatively pure (>80%) steel fractions because the distance between the magnet and the feed is well-defined. They also perform well if the feed contains a lot of fines or dust: non-magnetic dust is left on the belt. Cross belt separators can be mounted above practically all type of standard conveyors. Care should be taken to avoid steel parts (non-magnetic stainless is allowed) of the installation in the field of the magnet, since such steel parts will become magnetized and start to attract ferrous parts from the feed. Installing a magnet over a vibratory feeder is not recommended: bearings may become magnetized and show excessive wear, whereas the motion of the feeder itself is reduced because a magnetic field tends to counteract the motion of large metal structures (even if it is made from stainless steel).

MS.1.4.2. Line belt

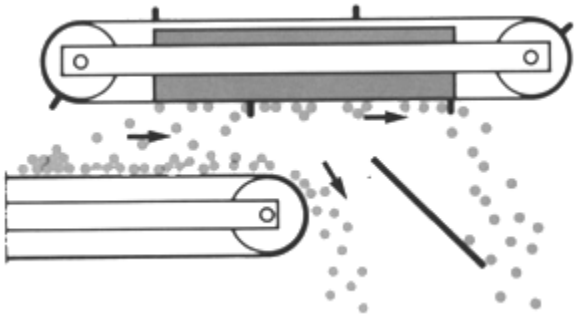

Fig. MS.10 – Principle of line belt magnetic separation. See also Fig. MS.1.

The principle is the same as that of the cross belt separator, but the ferrous metal is conveyed away from the end of the feed conveyor in the same direction. The same separators can be mounted as cross or line belt separators, however for large capacities line belt separators match the conveyor width and utilise the full width, contrary to cross belt separators. An important factor is the adjustment of the height. This strongly determines grade and recovery of the ferrous product.

For fluctuating feed, showing height fluctuations on the feed conveyor, separators that automatically adjust height by means of hydraulics are available. Heavy duty separators have a belt equipped with liner plates, e.g. for removal of coarse metal scrap from domestic waste. Multi stage magnetic separation is applied for battery pre-concentration from domestic waste. Here successive separators have a different height. The first separator removes ferrous without the weaker magnetic batteries, and the second separator that is mounted at a lower height removes a product that is enriched in batteries.

MS.1.4.3. Magnetic pulley separators

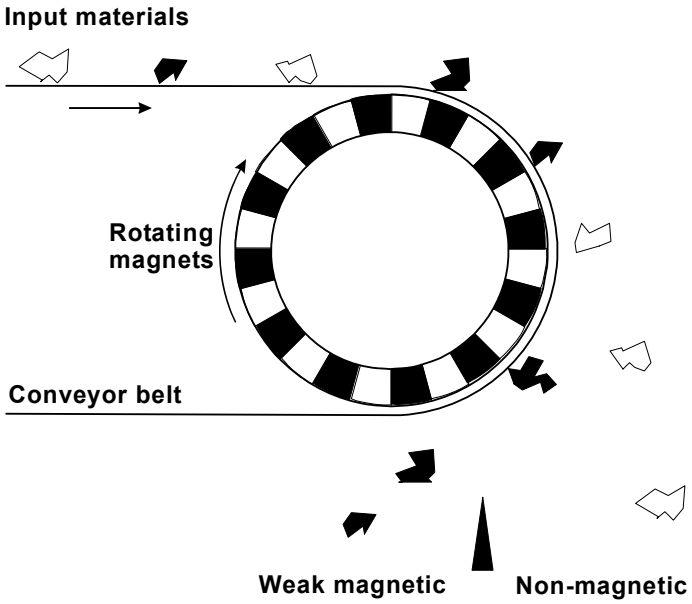

Fig. MS.11 - A magnetic pulley separator with permanent magnets

The functioning of a magnetic pulley separator is obvious from Fig. MS.11. Grade and recovery can be adjusted to some degree by changing:

- The splitter plate position dividing the two streams, allowing particles loosely attached to the roll just to fall in one or the other compartment.
- The rotation speed of the roll. At a higher speed loosely attached weakly magnetic particles have a higher tendency to fall off in the non-magnetic compartment by the action of centrifugal forces.

This design is very suitable as high intensity magnetic separator when strong magnets in a high gradient configuration are applied and belt speed is low (< 1 m/s). The pulley separator is relatively sensitive to particle size.

MS.1.4.4. Magnetic drum separators

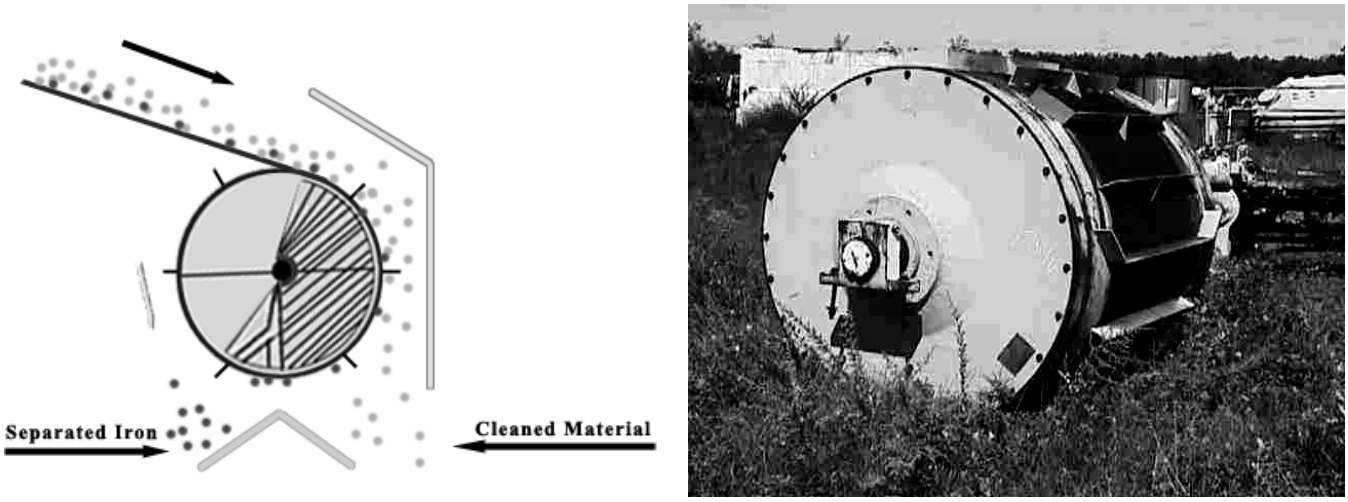

Fig. MS.12 – Magnetic drum separator

The principle is the same as that of the belt separators. In a rotating hollow drum one part is occupied by a permanent magnet (Fig. MS.12). The drum is equipped with baffles carrying the ferrous to the part of the drum outside the magnetic field. This design is very suitable for ferrous scrap separation in large volumes. An advantage is that the magnet is fully encapsulated preventing the build-up of magnetic fines onto to magnet, and the fact that there is no wear, maintenance, and supervision needed of an additional belt.

1.5 High intensity magnetic separators for metals

In general, magnetic separators for metals can be divided into two groups: low intensity and high intensity.
High intensity magnetic pulleys are suitable for the concentration of weakly magnetic stainless steels and particles that contain only some percentage of ferrous metal (e.g. plastics with a nail or irony aluminium, a complex material consisting of aluminium and mechanically connected magnetic parts such as iron bolts. In general, the high intensity magnetic separator is necessary in eddy current plants to protect the downstream eddy current systems against mechanical damage.

In separation of weakly magnetic materials, such as stainless steel, a combination of high gradient and high intensity magnetic field has to be realised to induce sufficient force in a particle. In Fig. MS.11 a schematic view is given of a separator for weak magnetic materials. The Nd-Fe-B permanent magnets on the drum are of alternating polarity and are 10-50mm thick. The belt operates at a speed of 0.3 to 0.6 m/s in order to reduce the radial forces on the particles when the belt passes over the magnetic pulley. In practice, about 50 percent of the stainless steel present in the heavy non-ferrous fraction of post-shredder material can be recovered with this type of magnetic separator.

With electromagnets it would be possible to generate very strong fields at a greater distance from the surface of the magnet compared to the standard cross and line belt separators. However, with modern rare earth magnets based on Nd-Fe-B, (neodymium, iron, and boron), strong fields can be obtained at low cost per volume of magnetic field. At present, 1 kg of installed Nd-Fe-B costs about €200 (or €1500 per dm^3), and production costs are further decreasing and magnetic properties improving. Therefore the magnetic separators based on permanent magnets are replacing electro-dynamic separators. A permanent magnet 1 metre wide with a length of 0.3 m and a thickness of 5 cm represents about 15 dm^3 or €25,000. At 10kW/hour per € this means that for a 40kW electrodynamic-magnet can be operated for 8000 hours or about 1 year for the separation of magnetic materials.

Broadly speaking, for materials smaller than 100 mm, magnetic separators based on permanent magnets can be used, representing the majority of post-shredder materials.

1.6. Wet magnetic medium recovery

High intensity magnetic separators are essential for the recovery of magnetite and ferrosilicon from heavy media separation plants. The principle is the same as the drum separator (Fig. MS.13). The difference is that the feed is wet slurry of very fine magnetite or ferrosilicon to be thickened for reuse in the heavy medium circuit. Maximum feed size is about 6 mm, but a typical heavy medium is usually much finer (0.05 – 0.1 mm).

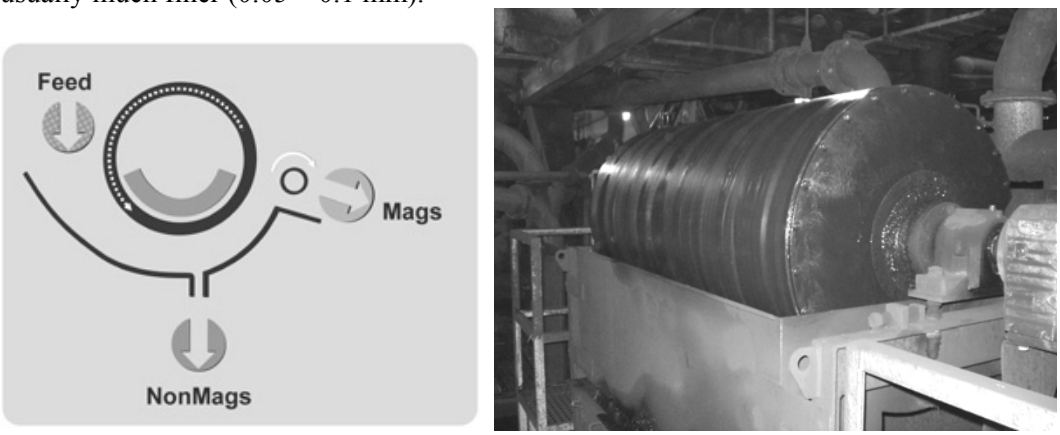

Fig. MS.13 – Wet magnetic separator for fine heavy medium recovery.

Most common is the co-current arrangement where the direction of flow of the slurry is the same as the rotation direction of the drum. This allows a high medium recovery. In a counter current arrangement recovery can be even higher, but there is a danger that non-magnetic material is trapped between the magnetic material in the zones of high concentration at the feed entry, lowering the grade.

1.7. Determination of χ

The majority of magnetic separations in recycling are carried out for the concentration of metals. For this it is in general not necessary to determine the magnetic susceptibility χ. This is however useful when weakly and non-magnetic materials are considered for separation. This proves useful in soil cleaning and may be of relevance for fine fractions of building materials waste. The separation of brickwork from concrete is considered, albeit in an experimental stage. Another application could be the concentration of certain organic mixtures. When the separation based on susceptibility differences proves useful it is important to realise that, apart from ferro-magnetic materials, only separation of fines (in general < 2mm) will be possible using dry or wet HGMS (High Gradient Magnetic Separation). A solution for larger sized material (>8 mm) is to electronically detect differences in χ and automatically sort afterwards. The procedure below can be applied to determine χ of unknown material, on condition it is fine (< 2 mm). Therefore grinding and classification must be applied first when needed. The separability of para- and non-magnetic materials can be determined with the Frantz Isodynamic Separator (FIS). It can be used as well for the determination of χ of unknown material. The FIS is a laboratory device. Due to high energy use and low capacity it cannot be applied for separations on practical scale. For this the use of HGMS should be considered.

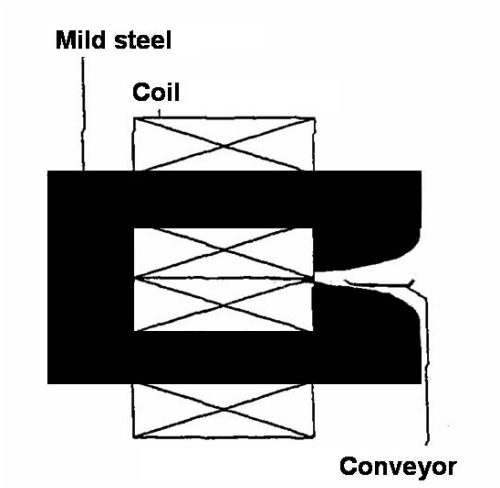

Fig. MS.14 – Frantz Isodynamic Separator (FIS)

The FIS consists of a high power electromagnet with two elongated poles (Fig. MS.14). Between the poles a narrow vibratory conveyor is mounted. The poles have a defined shape that causes a constant gradient of H^2 around the conveying zone. The material is moved at constant speed and undergoes a constant magnetic force between the poles. The material ends up in one of the two different bins at the end of the conveyor (Fig. MS.14, right). A separation can be achieved depending on feed and on separator adjustments, being tilt angle α and current strength I. The constant magnetic force F_{magn} is given by:

$$F_{magn} = c \cdot \chi_v \cdot V \cdot I^2 \qquad [MS.1.16]$$

By tilting the device with a tilt angle α backward, F_{magn}, directed outward, is countered by the gravity component in the inward direction F_g:

$$F_g = V \cdot \rho \cdot g \cdot \sin(\alpha) \qquad [MS.1.17]$$

This is the case when the material is spread evenly across the width of the conveyor. This can be achieved by adjustment of α and/or I. In this case in each bin the same amount of material will be present.

Symbols:

ρ	= material density [kg/m^3]	
α	= tilt angle	
χ	= (volume) susceptibility [-]	
χ_s	= specific or mass susceptibility = χ/ρ [m^3/kg]	
I	= current strength [A]	
V	= particle volume [m^3]	
c	= constant	

At the balance of F_g and F_{magn}:

$$\chi_m = f \cdot \frac{\sin(\alpha)}{I^2} \qquad [MS.1.18]$$

with f a separator constant given by the manufacturer.

1.8. HGMS

In the case a separation of materials belonging to the paramagnetic group needs to be made on an industrial scale it can be done by either dry or wet High Gradient Magnetic Separation. Fig. MS.15 shows a wet Jones HGMS originally developed for iron ore, but also applied for soil cleaning. For dry HGMS a prior drying step is required if the feed is not entirely dry and free flowing (thus in the case of damp feed). For more information we refer to minerals processing literature (Svoboda, 2003).

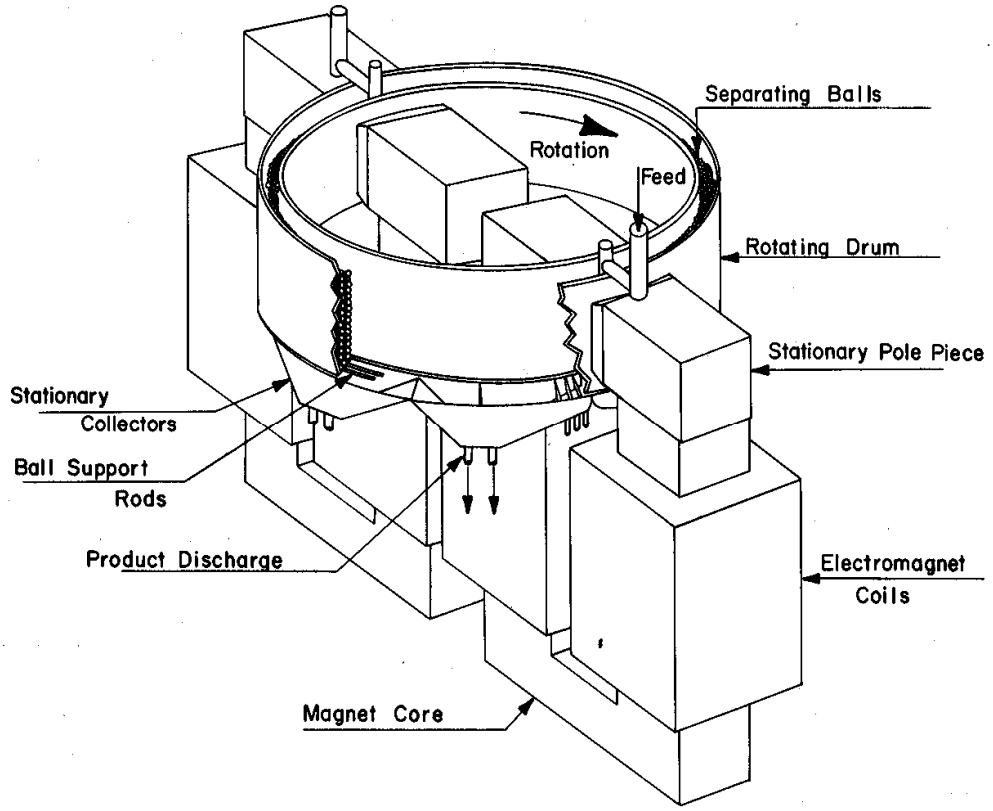

Fig. MS.15– Jones wet HGMS was developed for iron ore concentration but is also applied for soil cleaning